

## SIRLE LIIVAMÄGI

Neoproterozoic Baltic paleosol:  
geology and paleoenvironmental  
interpretation





## **SIRLE LIIVAMÄGI**

Neoproterozoic Baltic paleosol:  
geology and paleoenvironmental  
interpretation



1632

UNIVERSITY OF TARTU  
PRESS

Department of Geology, Institute of Ecology and Earth Sciences, Faculty of Science and Technology, University of Tartu, Estonia

This dissertation is accepted for the commencement of the degree of Doctor of Philosophy in Geology at the University of Tartu on 16<sup>th</sup> March 2015 by the Scientific Council of the Institute of Ecology and Earth Sciences, University of Tartu.

Supervisors: Kalle Kirsimäe and Peeter Somelar  
Department of Geology, University of Tartu, Estonia

Opponent: Dr. Steven G. Driese  
Department of Geology, Baylor University, U.S.A.

This thesis will be defended at the University of Tartu, Estonia, Chemicum, Ravila 14A, room 1019, on the 18th of June 2015 at 12:15.

Publication of this thesis is granted by the Institute of Ecology and Earth Sciences, University of Tartu and by the Doctoral School of Earth Sciences and Ecology created under the auspices of the European Social Fund.



European Union  
European Social Fund



Investing in your future

ISSN 1406-2658  
ISBN 978-9949-32-806-2 (print)  
ISBN 978-9949-32-807-9 (pdf)

Copyright: Sirle Liivamägi, 2015

University of Tartu Press  
[www.tyk.ee](http://www.tyk.ee)

# CONTENTS

LIST OF ORIGINAL PUBLICATIONS .....	6
1. INTRODUCTION.....	7
2. GEOLOGICAL SETTING .....	9
3. MATERIAL AND METHODS .....	12
4. RESULTS .....	15
4.1. Petrographical characterization and alteration zones of the weathering profiles.....	15
4.2. Mineralogical characterization of the weathering profiles .....	17
4.2.1. Whole-rock mineralogy.....	17
4.2.2. Clay mineralogy .....	20
4.2.3. Scanning electron microscopy.....	20
4.3. Geochemical characterization of the weathering profiles .....	23
5. DISCUSSION .....	27
5.1. Preservation, weathering maturity and influence of diagenetic overprint.....	27
5.2. Age, paleoclimatological–paleogeographical interpretation and implications of the Baltic paleosol .....	30
6. CONCLUSIONS .....	36
REFERENCES .....	38
SUMMARY IN ESTONIAN .....	45
ACKNOWLEDGEMENTS .....	48
PUBLICATIONS .....	49
CURRICULUM VITAE .....	91
ELULOOKIRJELDUS.....	92

## LIST OF ORIGINAL PUBLICATIONS

This thesis is based on the following published papers, which are referred to in the text by their Roman numerals. The papers are reprinted by kind permission of the publishers.

- I** **Liivamägi, S.**, Somelar, P., Mahaney, W.C., Kirs, J., Vircava, I., Kirsimäe, K., 2014. Late Neoproterozoic Baltic paleosol: Intense weathering at high latitude? *Geology* 42, 323–326.
- II** **Liivamägi, S.**, Somelar, P., Vircava, I., Mahaney, W.C., Kirs, J., Kirsimäe, K., 2015. Petrology, mineralogy and geochemical climofunctions of the Neoproterozoic Baltic paleosol. *Precambrian Research* 256, 170–188.
- III** Vircava, I., Somelar, P., **Liivamägi, S.**, Kirs, J., Kirsimäe, K., 2015. Origin and paleoenvironmental interpretation of aluminum phosphate–sulfate minerals in a Neoproterozoic Baltic paleosol. *Sedimentary Geology* 319, 114–123.

### Author's contribution

Paper I: The author was responsible for planning original research, data collection, X-ray diffraction analyses and interpretation of analytical results, mass-balance modeling of weathering processes, synthesis of mineralogical-geochemical analytical data and writing the manuscript.

Paper II: The author was responsible for planning original research, data collection, X-ray diffraction, X-ray fluorescence and scanning electron microscope analyses and interpretation of analytical results, mass-balance modeling of weathering processes, synthesis of different analytical results and writing the manuscript.

Paper III: The author was responsible for petrographical and mineralogical analyses and interpretation of analytical results and contributed to the writing of the manuscript.

# I. INTRODUCTION

Paleosols are remains of ancient soils. They are formed at the Earth's surface either during periods of landscape stability or in terrestrial depositional systems as long as the rate of sedimentation does not exceed the rate of pedogenesis. Paleosols are developed in direct contact with climatic and environmental conditions that existed at the time of soil formation and they hold potentially important information of past environments. The first studied paleosols were described in the Quaternary record, now, however, they are commonly recognized in strata as old as the Precambrian. With new quantitative techniques (e.g. whole-rock and isotopic geochemistry) it is possible to interpret their formation without the "nearest living relative" comparison (e.g. Retallack, 1992; Kraus, 1999; Sheldon and Tabor, 2009). Interest in pre-Quaternary paleosols, especially in paleosols that formed at the Archean–Proterozoic and Proterozoic–Paleozoic transitions are of special interest because they have proved to be beneficial for solving diverse geological problems (e.g. Retallack, 2012, 2013a,b) and could reflect the evolution of atmospheric oxygenation in symbiosis with bioevolution (Campbell and Squire, 2010; Och and Shields-Zhou, 2012). The role of Precambrian weathering crusts as indicators of primitive soil ecosystems and climatic conditions has been questioned by many researchers (e.g. Sutton and Maynard, 1996; Medaris et al., 2003), because they have a low preservation potential, tend to be deformed, diagenetically altered and/or metamorphosed to a different level (Retallack, 1992), and can be easily confused with alteration zones caused by groundwater or hydrothermal activity (e.g. Maynard, 1992; Nedachi et al., 2005). Driese et al. (2007), however, have shown that despite possible hydrothermal and diagenetic alteration, the Proterozoic–Phanerozoic terrestrial paleoweathered surfaces which developed on the granitic basement are remarkably similar to modern weathering profiles and can provide important evidence for early weathering conditions.

The transition from the Proterozoic to Phanerozoic (ca. 1000–500 Ma) was a time of significant environmental changes including extreme reconstructions in the Earth's biogeochemical cycles and disturbances in the carbon cycle (Halverson and Shields-Zhou, 2011), global glaciation events, followed by episodic warm and humid periods (Harland, 2007; Pierrehumbert et al., 2011), final oxygenation of the atmosphere (Och and Shields-Zhou, 2012) and the emergence of multicellular animal life (Narbonne, 2005). The Proterozoic–Phanerozoic boundary is marked by a widespread erosional unconformity called the Great Unconformity which is preserved as a continental denudation surface while the weathering crust itself is rarely preserved (Peters and Gaines, 2012). It is found in all major continents of that time – Avalonia, Baltica, Gondwana, Laurentia and Siberia (Brasier, 1980; Avigad et al., 2005; Peters and Gaines, 2012). The formation of the Great Unconformity in the Neoproterozoic represents a significant and intriguing change in the mineralogical evolution on the Earth (Hazen et al., 2008, 2013). The large-scale chemical weathering

during the formation of the Great Unconformity evidently influenced the seawater chemistry and global biogeochemical cycling and may have been an environmental trigger for the evolution of biomineralization and the “Cambrian life explosion” (Peters and Gaines, 2012).

Precambrian paleosols have a low preservation potential and weathering events are typically preserved as denudation surfaces, rather than weathering crusts (Retallack, 1992; Peters and Gaines, 2012). As a consequence, the influence of Neoproterozoic climatic disturbances on continental weathering patterns and paleosol morphogenesis is not well known. Climatic fluctuations in the Neoproterozoic, characterized by cool climate snowball glaciations and warm and humid greenhouse periods when exceptionally high CO<sub>2</sub> levels accumulated over glacial periods may have triggered intensified continental weathering, which subsequently caused drawdown of atmospheric CO<sub>2</sub> (Harland, 2007; Pierrehumbert et al., 2011). This is evidenced by a strong increase in chemical weathering indices in non-glacigenic marine successions subsequent to the deposition of glacigenic sediments (Rieu et al., 2007a,b), but the continental evidence of intensified weathering episodes in the Neoproterozoic is scarce.

The deeply weathered and unmetamorphosed Neoproterozoic paleoweathered crust (hereafter Baltic paleosol *sensu* Liivamägi et al., 2014 – PAPER I), forms a major disconformity in the eroded Paleoproterozoic–Mesoproterozoic metamorphic–plutonic crystalline basement, overlain by 100–2500 m thick Ediacaran–Paleozoic sedimentary rocks of the East European Platform at the southern margin of the Fennoscandian Shield of the former Baltica continent. It is possibly one of the few well-preserved examples of paleosol morphogenesis of late Precambrian time and therefore useful for reconstructing the paleoclimate and -environments of the Neoproterozoic, the time when the modern world emerged. This thesis addresses the geology and paleoenvironmental interpretation of the Baltic paleosol sequence.

The aims of the thesis are:

1. to study the petrographical, (clay)mineralogical and geochemical composition of the Baltic paleosol in order to determine the preservation, weathering maturity and possible diagenetic overprint(s) of this Precambrian paleosol;
2. to model geochemical climofunctions in order to determine the environmental conditions at the time of paleosol formation.



## 2. GEOLOGICAL SETTING

The Baltic paleosol developed on the crystalline basement in the north-western part of the Russian Platform of the East European Craton, at the southern margin of the Baltic Shield, Baltic Basin. The study area is located in northern and western Estonia (Figure 1). The Paleoproterozoic crystalline basement in Estonia represents the ca. 1.9–1.7 Ga old orogenic Svecofennian Domain (Puura and Huhma, 1993; Kirs et al., 2009). It is composed of metasedimentary and metavolcanic rocks, regionally metamorphosed to amphibolite and granulite facies and is intersected by 1.6–1.4 Ga Paleo-Mesoproterozoic anorogenic plutonic rapakivi granites (Haapala et al., 2005; Kirs et al., 2009).

Deeply metamorphosed and migmatized sedimentary and volcanic orogenic rocks are divided into six petrological–structural zones. The northern part of Estonia is represented by amphibolites and biotite–amphibole gneisses of the Tallinn zone, high-alumina gneisses of the Alutaguse zone (NE Estonia) and amphibolites and biotite–amphibole gneisses of the Tapa zone. The small E–W-trending Jõhvi zone is located in the NE part of the Alutaguse zone and consists of various pyroxene and garnet-bearing gneisses together with magnetite-rich quartzites metamorphosed to granulite facies. Radiogenic ages of ca. 1.9–1.8 Ga of the northern Estonian complexes are correlated with the volcanic arc supracrustal rocks of the Fennian orogen in southern Finland (Soesoo et al., 2004; Kirs et al., 2009; Lahtinen and Nironen, 2010). The West Estonian zone and the South Estonian zone contain amphibolites, biotite–amphibole–pyroxene and biotite–feldspar gneisses of the granulite facies of the Estonian–Latvian Granulite Belt. The U–Pb zircon ages of 1.8 Ga and less of south-western complexes allow their correlation with the volcanic arc formations of the Svecobaltic orogen extended from south-eastern Sweden (Kirs et al., 2009). The Sigula monzogabbro intrusion in northern Estonia and the Riga rapakivi batholith in south-western Estonia represent an episode of bimodal anorogenic rapakivi magmatism, which reflects an intercontinental extensional tectonic setting of the area 1630–1580 Ma ago (Rämö et al., 1996). The youngest rock suits in the crystalline basement are ca. 600–595 Ma old foiditic dykes intersecting the anorogenic Riga pluton and lavas lying on the eroded surface of the rapakivi granites in western Latvia (Bogatikov and Birkis, 1973; Brangulis, 1985).

A series of shear and cataclastic fault zones are located all over the Precambrian basement area. The main tectonic boundary is the NW–SE-striking and about 70° SW aligned Paldiski–Pihkva shear/thrust zone separating the S–SW Estonian granulitic and N–NE Estonian amphibolitic facies. The other deep crustal shear zone is the W–E-striking, nearly vertical Middle Estonian fault zone that intersects the Paldiski–Pihkva fault zone and has cataclased some small postorogenic plutons in central Estonia, therefore indicating activity during post- and anorogenic basement block movements ca. 1.6–1.5 Ga (Soesoo et al., 2004).

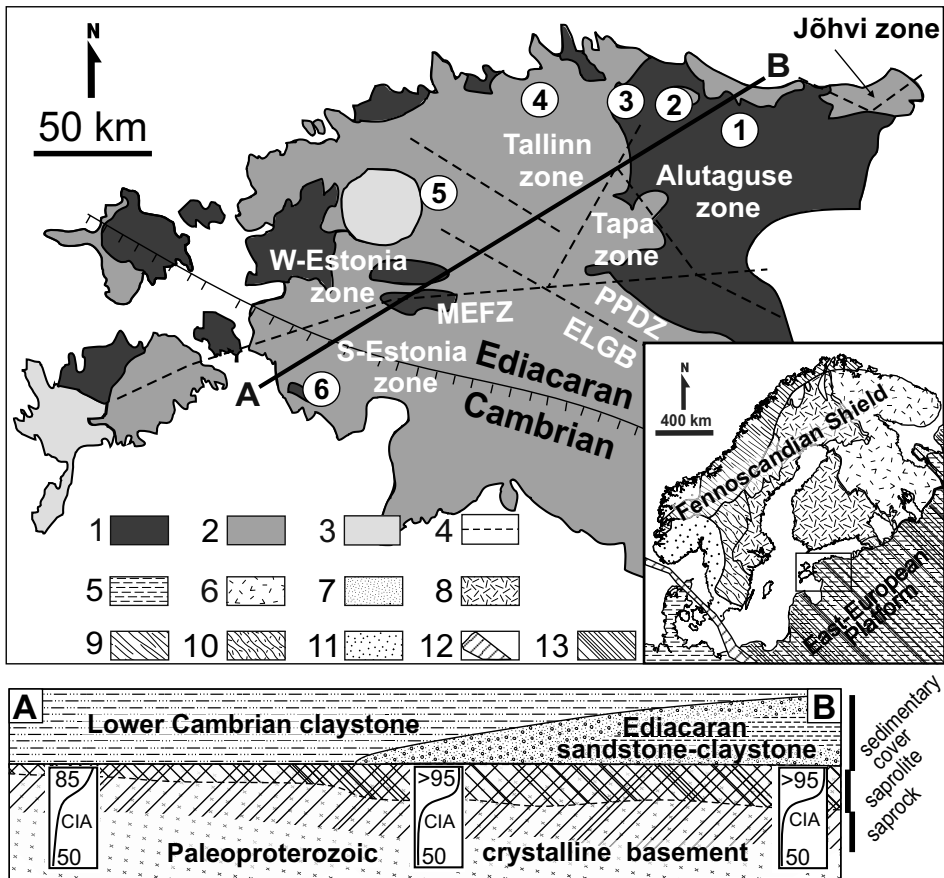


**Figure 1.** Simplified geological setting of the crystalline basement of the study area, schematic cross section (not to scale) of the Baltic paleosol and locations of the studied weathering profiles: 1. Varja (F195), 2. Pada-Aru (F185), 3. Nudi (F266), 4. Sigula (F124), 5. Lohu (F280), 6. Varbla (502). Legend: 1 – metasedimentary rocks, 2 – metavolcanics, 3 – rapakivi granites, 4 – shear or thrust zones, 5 – Phanerozoic, 6 – Archean, 7 – Ediacaran, 8 – Svecofennian Domain, 9 – Caledonides, 10 – Transscandinavian Igneous Belt, 11 – Sveconorwegian Domain, 12 – Tornquist Line, 13 – distribution of the Baltic paleosol. PPDZ – Paldiski–Pihkva Deformation Zone, MEFZ – Middle Estonian Fault Zone, ELGB – Estonian–Latvian Granulite Belt (after Papers I and II – Liivamägi et al., 2014, 2015).

The Fennoscandian sub-Cambrian/Ediacaran peneplain was formed during the late Paleoproterozoic and early Mesoproterozoic when the Svecofennian juvenile crust was subjected to extensive denudation (Kohonen and Rämö, 2005). The upper part of the peneplained crystalline basement is strongly affected by chemical weathering. A few to tens of meters (up to 150 m in fractured fault zones) thick weathered crust/Baltic paleosol (Figure 1) is found below the Ediacaran sandstones–claystones in eastern and central Estonia and

Cambrian claystones and silt- and sandstones in western Estonia (Kuuspalu et al., 1971; Puura et al. 1983; Vanamb and Kirs, 1990; Mens and Pirrus, 1997). The peneplain of the crystalline basement and sedimentary formations on top of the basement are gradually sloping 2–4 m/km towards the south to a depth of about 100 m in northern Estonia and >700 m in southern Estonia and northern Latvia. The Baltic paleosol continues to exist to the east in north-western Russia and to the south at about 700–1500 m under Phanerozoic sediments in Latvia (Bogatikov and Birkis, 1973; Brangulis, 1985; Koistinen et al., 1996) and 1200–2900 m in Kaliningrad District, Russia (Meshcherskii et al., 2003).

### 3. MATERIAL AND METHODS

The Baltic paleosol does not outcrop on the surface but can be recovered from drillcores below conformably overlying Ediacaran–Paleozoic sediments. The core sections from the Varja (F195), Pada-Aru (F185), Nudi (F266), Sigula (F124), Lohu (F280) and Varbla (502) drill holes were selected for petrological, mineralogical and geochemical studies. These core sections represent different parent rock types found in the crystalline basement of the study area and contain the uppermost at least partially preserved kaolinite-rich horizons. The studied sections are located in the northern and western parts of Estonia (Figure 1) and the thickness of the Baltic paleosol in these sections varies from ca. 7 m in the Varbla (502) core and 24 m in the Varja (F195) core up to ca. 40 m in the Lohu (F280), Nudi (F266) and Sigula (F124) cores and ca. 50 meters in the Pada-Aru (F185) core. In most cases the sampling interval spans from practically unaltered crystalline rocks up to highly altered saprolitic (kaolinite-rich) paleosol horizons. Altogether 147 samples were collected and analyzed by means of petrographical, mineralogical and geochemical methods.

For micromorphology and mineral alteration analysis fresh to highly weathered sections were selected from the Varja (F195), Pada-Aru (F185), Sigula (F124) and Lohu (F280) drillcores. Selected samples were impregnated with thin epoxy resin, then polished and inspected using a variable pressure Zeiss EVO 15MA scanning electron microscope (SEM). The element distribution maps and chemical composition of the phases were collected using Oxford AZtec X-Max energy dispersive spectrometer (EDS) and Wave700 wavelength dispersive spectrometer (WDS) systems. Carbon coated samples were imaged and analyzed in high vacuum mode. The morphology of authigenic mineral phases was inspected in freshly broken surfaces of selected samples from the Sigula (F124) drillcore with thin Pt coating (ca. 5 nm).

The mineralogical composition of whole-rock samples was studied by means of X-ray diffractometry (XRD). Samples from the Varja (F195), Pada-Aru (F185), Nudi (F266), Sigula (F124), Lohu (F280) and Varbla (502) profiles were pulverized in a planetary mill and unoriented preparations were made. The XRD patterns were collected on a Bruker D8 Advance diffractometer using  $\text{CuK}\alpha$  radiation and a LynxEye positive sensitive detector in the  $2\text{--}70^\circ$   $2\theta$  range. The quantitative mineralogical composition of the samples was interpreted and modeled by the Rietveld algorithm-based program Siroquant-3 (Taylor, 1991).

The mineralogical maturity was estimated using the mineralogical index of alteration (MIA; Johnsson, 1993; Nesbitt et al., 1996), a dimensionless number between 0 and 100, calculated from mineral weight percentages derived from XRD analysis:

$$\text{MIA} = [\text{quartz} / (\text{quartz} + \text{K-feldspar} + \text{plagioclase})] \times 100.$$

The clay fraction (<2  $\mu\text{m}$ ) was separated using standard sedimentation procedures and oriented clay mineral slides were prepared for samples selected from the Sigula (F124) core. The XRD patterns in air-dry (AD) and ethylene glycol saturated (EG) states from oriented preparations were collected on the Bruker D8 Advance diffractometer using  $\text{CuK}\alpha$  radiation and LynxEye positive sensitive detector in the  $2\text{--}45^\circ$   $2\theta$  range. The XRD patterns were modeled, in both AD and EG states, using the Sybilla<sup>©</sup> software developed by Chevron<sup>™</sup> (Aplin et al., 2006).

The geochemical compositions of the Pada-Aru (F185), Nudi (F266) and Lohu (F280) profiles were determined using ICP-OES analysis at the Acme Analytical Laboratory, Canada. The geochemical compositions of the Sigula (F124), Varja (F195) and Varbla (502) profiles were determined by X-ray fluorescence spectrometry at the Department of Geology, University of Tartu using a Rigaku Primus II spectrometer.

Isocon analysis (Grant, 1986) and mass-balance calculations (Brimhall et al., 1988) were used to estimate major oxides depletion and enrichment trends with titanium as an immobile element. The reference point was chosen from the average of unaltered parent rocks as follows: 246–252 m depth for the Varja (F195), 248–254 m depth for the Pada-Aru (F185), 236–250 m depth for the Nudi (F266), 252–262 m depth for the Sigula (F124), 308 m depth for the Lohu (F280) and 528–530 m depth for the Varbla (502) profile.

The degree of chemical weathering was estimated using the chemical index of alteration (CIA, Nesbitt and Young, 1982), chemical index of alteration minus potassium (CIA – K, Maynard, 1992) and plagioclase index of alteration (PIA, Fedo et al., 1995) which are dimensionless numbers between 0 and 100. The indices were calculated using molecular proportions derived from major element geochemistry:

$$\text{CIA} = [\text{Al}_2\text{O}_3 / (\text{Al}_2\text{O}_3 + \text{CaO}^* + \text{Na}_2\text{O} + \text{K}_2\text{O})] \times 100;$$

$$\text{PIA} = [(\text{Al}_2\text{O}_3 - \text{K}_2\text{O}) / (\text{Al}_2\text{O}_3 + \text{CaO}^* + \text{Na}_2\text{O} - \text{K}_2\text{O})] \times 100,$$

where  $\text{CaO}^*$  is the amount of CaO combined in the silicate fraction of the rock. The index CIA – K is calculated similarly to CIA except that  $\text{K}_2\text{O}$  is not used.

Samples with high CIA values (>85) and without traces of carbonate minerals (calcite, dolomite, siderite) and apatite (Ca-phosphate), as confirmed by XRD analysis, were used for climatological reconstructions. The CIA – K (Sheldon et al, 2002) and CALMAG (Nordt and Driese, 2010) indices were used to estimate mean annual precipitation (MAP), and salinization (Sheldon et al., 2002) and clayeyness (Sheldon, 2006b) molecular weathering ratios were used to estimate mean annual temperature (MAT).

The relationship between CIA – K and MAP is found using an exponential fit:

$$\text{MAP} = 221e^{0.0197(\text{CIA} - \text{K})},$$

where the standard error (ER) is  $\pm 172$  mm and  $R^2 = 0.73$  for the empirical fit.

The relationship between CALMAG and MAP is found with the equation:

$$\text{MAP} = 22.69 \times (\text{CALMAG}) - 435.8,$$

where ER is  $\pm 108$  mm,  $R^2 = 0.90$  and CALMAG is a dimensionless number calculated as follows:  $\text{CALMAG} = \text{Al}_2\text{O}_3 / (\text{Al}_2\text{O}_3 + \text{CaO} + \text{MgO}) \times 100$ .

The relationship between MAT and salinization (S) is found with the equation:

$$T = -18.516 \times (S) + 17.298,$$

where RE =  $\pm 4.4$  °C,  $R^2 = 0.37$  and  $S = \text{K}_2\text{O} + \text{Na}_2\text{O} / \text{Al}_2\text{O}_3$ .

The relationship between MAT and clayeyness (C) is found with the equation:

$$T = 46.94 \times (C) + 3.99,$$

where RE =  $\pm 0.6$  °C and  $R^2 = 0.96$  and  $C = \text{Al}_2\text{O}_3 / \text{SiO}_2$ .

The geochemical composition of aluminum phosphate–sulfate (APS) minerals was obtained by microprobe analyses of APS minerals, where 11 crystals and crystal aggregates of  $>5$   $\mu\text{m}$  size were studied. The structural formulae of APS minerals were calculated on the basis of normalization on 14 oxygen atoms. Si, K and Fe were excluded from calculations because of contamination from the surrounding matrix. The data were normalized to 85% anhydrous total (Gaboreau et al., 2005) and alumina was corrected according to the method described in Scott (1987). The idealized general formula of the APS mineral is  $\text{AB}_3(\text{XO}_4)_2(\text{OH})_6$ , where the A site can be occupied by either monovalent, divalent, trivalent or even tetravalent cations such as  $\text{K}^+$ ,  $\text{Na}^+$ ,  $\text{Ca}^{2+}$ ,  $\text{Sr}^{2+}$ ,  $\text{Ba}^{2+}$  or  $\text{REE}^{3+}$ , the B site is mostly occupied by cations  $\text{Al}^{3+}$  or  $\text{Fe}^{3+}$  and the anion X site is occupied by either  $\text{S}^{6+}$ ,  $\text{P}^{5+}$ ,  $\text{As}^{5+}$ ,  $\text{Cr}^{6+}$ ,  $\text{Sb}^{5+}$  or  $\text{Si}^{4+}$  (Scott, 1987).

## 4. RESULTS

### 4.1. Petrographical characterization and alteration zones of the weathering profiles

The Pada-Aru profile (F185; Liivamägi et al., 2014, 2015 – PAPERS I, II) is developed in late orogenic metagabbroic rocks intersected by migmatite–pegmatite veins in the Pada massif and can be subdivided into parent rock and three weathered zones (Figure 2). The lowermost greenish-black zone 30–50 m below the weathered surface represents parent rock and a lower saprock section with the original amphibolitic–gabbroic rock structure preserved. The weathering phenomena in this zone are observed only along (micro)fractures and within intersecting sparse fracture planes/surfaces. The middle greenish-gray and reddish-gray zone 10–30 m below the weathered surface represents a moderately to strongly weathered saprock section where the original rock structure is preserved but primary minerals are replaced by clay and authigenic Fe-mineral masses. The saprock section grades into the uppermost 10 m thick reddish and strongly weathered saprolite zone where the initial structure of the parent rock is unrecognizable and the paleosol is composed of friable clayey material.

The Sigula profile (F124; Liivamägi et al., 2015 – PAPER II) is developed in the post-orogenic metagabbroic Sigula massif and can be subdivided, similarly to the Pada-Aru profile, into a parent rock and three weathered zones (Figure 2). The lowermost greenish-gray zone 20–40 m below the weathered surface consists of fresh ophitic monzogabbroic parent rock and a lower saprock section where the original parent rock structure is completely preserved but weak traces of weathering occur along (micro)fractures. The lower saprock section is followed by moderately weathered greenish-gray and reddish saprock section which grades into the uppermost strongly weathered reddish friable and clayey saprolite, which is preserved only in a ca. 3 m thick zone.

The Lohu profile (F280; Liivamägi et al., 2014, 2015 – PAPERS I, II) is developed in migmatized amphibolitic rocks. This profile does not reach parent rock and the lowermost saprock zone and therefore it consists only of two weathered zones (Figure 2). The greenish-gray saprock section is slightly to moderately weathered with alteration halos extending from fracture planes into the rock for a few centimeters. The upper part of the saprock consists of strongly weathered, varicolored (reddish-greenish-white) gneisses which grade into clayey saprolite in the uppermost beds, in an about 6 m thick zone.

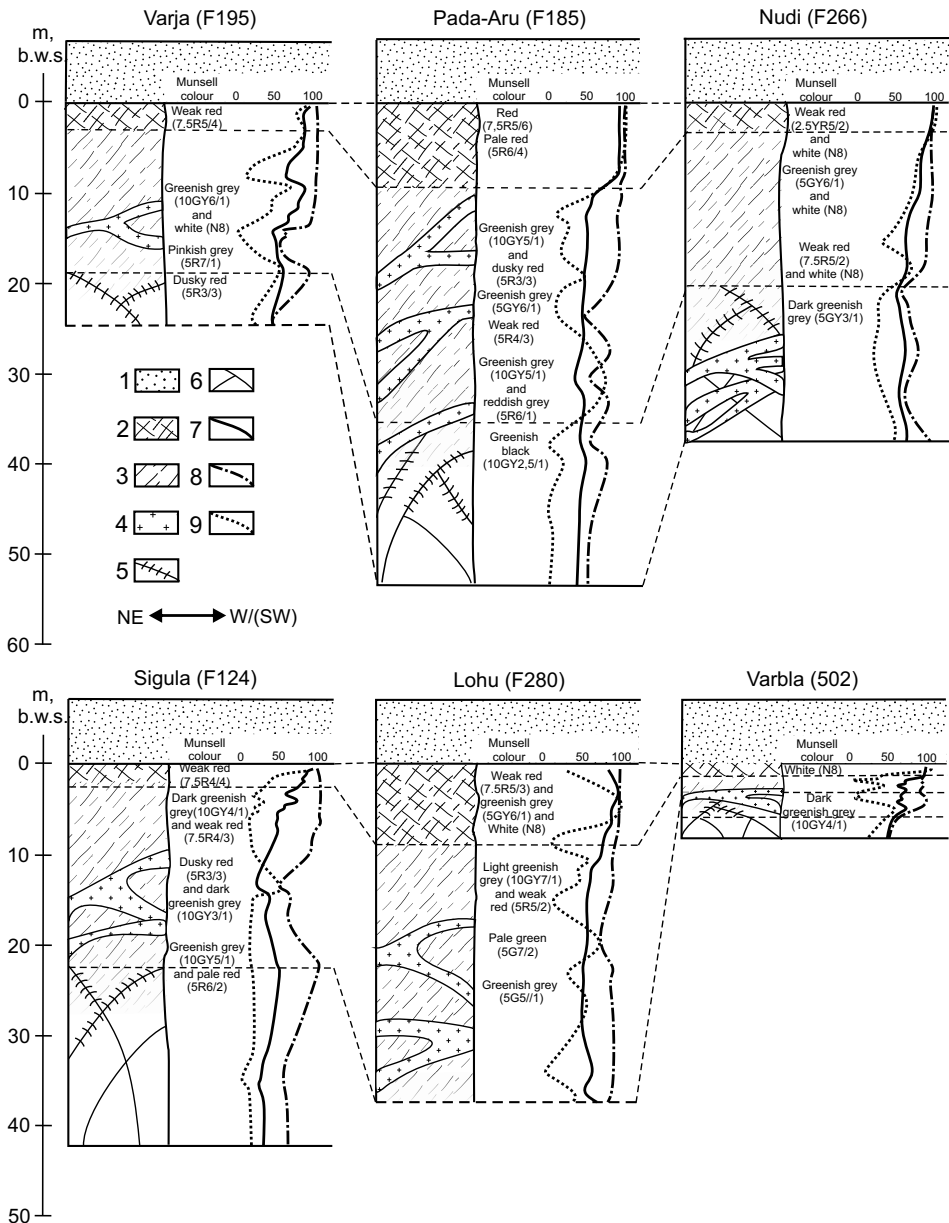


**Figure 2.** Weathered profile appearances of the Baltic paleosol with CIA, CIA – K and MIA representative graphs. Legend: 1 – Ediacaran–Cambrian sediments, 2 – saprolite, 3 – saprock, 4 – coarse-grained migmatite veins, 5 – slightly weathered parent rock, 6 – fresh parent rock, 7 – Chemical Index of Alteration, 8 – Chemical Index of Alteration minus Potassium, 9 – Mineral Index of Alteration (Paper II – Liivamägi et al., 2015).



The Nudi profile (F266; Liivamägi et al., 2015 – PAPER II) is developed in biotite–plagioclase gneisses and can be subdivided into parent rock and three weathered zones (Figure 2). The lowermost dark greenish-gray zone 20–40 m below the weathered surface represents parent rock and a lower saprock section with the original plagioclase–biotite gneissic rock structure, with occasional amphibole-rich layers, still preserved. The original structure of the parent rock, with only primary minerals replaced by clays, is still more or less preserved in the middle greenish-gray and reddish saprock zone, but it becomes unrecognizable in the uppermost ca. 3 m thick reddish colored clayey saprolite.

The Varja profile (F195; Liivamägi et al., 2015 – PAPER II) is developed in biotite–plagioclase gneisses and can be subdivided into three weathered zones. This core does not reach the unweathered parent rock (Figure 2). The lowermost part of the profile 20–25 m below the weathered surface and its middle part 4–20 m below the weathered surface consist of slightly to moderately weathered greenish-gray and reddish plagioclase–biotite gneisses with occasional amphibole-rich layers. The original structure in these zones is still visible. Strongly weathered reddish friable saprolite without any recognizable original rock structure is preserved in the uppermost ca. 4 m thick zone.

The Varbla profile (502; Liivamägi et al., 2015 – PAPER II) is developed in pyroxene gneisses and is much thinner than the other profiles, with overall thickness reaching only up to ca. 7 m (Figure 2). Nevertheless, the profile is rather well preserved and consists of parent rock, greenish-gray slightly to moderately weathered saprock where the original rock structure is still preserved and white ca. 1 m thick saprolite where the initial structure of the parent rock is completely lost.

## **4.2. Mineralogical characterization of the weathering profiles**

### **4.2.1. Whole-rock mineralogy**

The parent rock of all weathering profiles of the Baltic paleosol is characterized by an assemblage of quartz, feldspars (K-feldspar and/or plagioclase) and primary phyllosilicates (biotite and muscovite), and hornblende in more mafic parent rock. The rocks in weathering profiles themselves are represented by a clay mineral assemblage of chlorite, mixed-layer illite–smectite and chlorite–smectite, and kaolinite together with Fe-oxides/hydroxides, which are mainly represented by hematite and goethite (Figure 3; Liivamägi et al., 2014, 2015 – PAPERS I, II). The MIA values range from 87(97) up to 100 in the uppermost horizon of the saprolite sections in all weathering profiles studied (Figure 2; Liivamägi et al., 2015 – PAPER II).

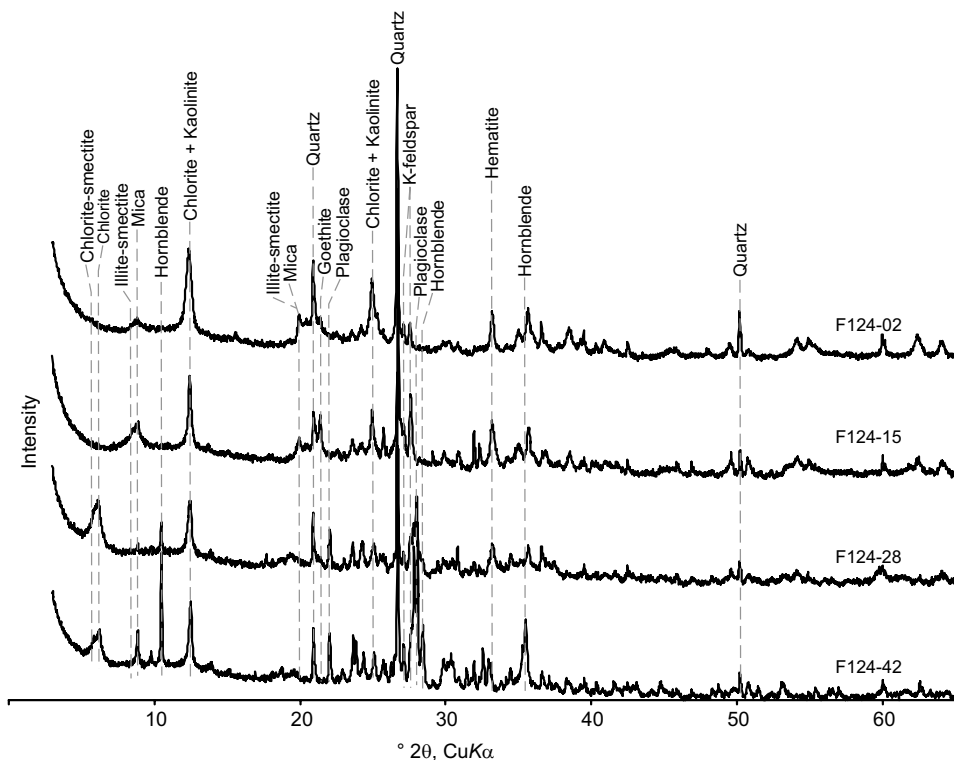


**Figure 3.** Representative randomly oriented X-ray diffraction patterns from the Sigula (F124) weathering profile (Paper II – Liivamägi et al., 2015).

The profiles that developed in amphibolitic and gabbroic rocks (Pada-Aru, Lohu and Sigula) are characterized by a rather thick uppermost kaolinite-rich saprolite zone. The kaolinite content in the thickest and best-preserved Pada-Aru (F185) profile reaches 60–72 wt% in an about 7 m thick horizon in the saprolite section with an associated goethite–hematite content reaching 23 wt% (Liivamägi et al., 2014, 2015 – PAPERS I, II). In the Sigula (F124) profile the kaolinite content reaches 55 wt% and the associated Fe-oxyhydroxides (hematite and goethite) compose 10–30 wt% of the crystalline phases in the about 3 m thick strongly weathered uppermost horizon (Liivamägi et al., 2015 – PAPER II). The uppermost 1.5 m thick saprolite horizon of the Sigula (F124) profile is peculiar for the presence of APS minerals which compose up to 4 wt% of the crystalline phases, whereas the APS phase content declines with the decreasing weathering intensity (Vircava et al., 2015 – PAPER III). In the Lohu (F280) profile the kaolinite content reaches 40–60 wt% and Fe-oxyhydroxides compose ca. 10 wt% of the crystalline phase in an about 6 m thick horizon (up to 23 wt% about 8 m below the paleoweathered surface) of the saprolite section (Liivamägi et al., 2014, 2015 – PAPERS I, II).

In the moderately weathered saprock section of the Pada-Aru (F185) and Sigula (F124) profiles the kaolinite and Fe-oxyhydroxides decline down-profile

and are subsequently replaced by mixed-layer illite–smectite, chlorite and chlorite–smectite minerals (up to 30 wt%). Feldspars, micas and hornblende are completely absent in the uppermost saprolitic kaolinite-rich zone of the Pada-Aru (F185) profile and appear in the saprock section: K-feldspar and micas ca. 10 m, and plagioclase and hornblende ca. 20 m below the paleoweathered surface. In the Sigula (F124) and Lohu (F280) profiles K-feldspar is practically absent in the uppermost saprolite section and its content increases towards the saprock section. Micas, plagioclase and hornblende are nearly absent in the Lohu (F280) profile. In the Sigula (F124) profile the first traces of micas appear ca. 3 m, plagioclase ca. 6 m and hornblende ca. 12 m below the paleoweathered surface. The parent rock with the amphibole–plagioclase assemblage becomes unaltered at ca. 20–30 m depth in all profiles (Liivamägi et al., 2014, 2015 – PAPERS I, II).

The uppermost kaolinite-rich saprolite section in the Nudi (F266) and Varja (F195) profiles that developed in gneissic basement rocks is 3–4 m thick. The kaolinite content reaches 30–50 wt% in these zones. The Fe-oxyhydroxides content in these sections, compared to the profiles developed in mafic parent rocks (Pada-Aru, Sigula and Lohu), remains relatively low, being up to ca. 14 wt% in the Varja (F195) and ca. 7 wt% in the Nudi (F266) profile. Both of these profiles are also characterized by a high residual quartz content (40–50 wt%) in the uppermost kaolinite-rich saprolite zone when compared to the profiles that developed in gabbroic rocks where the quartz content is only ca. 4–10 wt%. Other mineral trends show a similar behavior to the profiles that developed in the mafic parent rocks and kaolinite is down-profile gradually replaced by mixed-layer illite–smectite, chlorite and chlorite–smectite type clay phase. In the Varja (F195) profile K-feldspar and plagioclase become abundant at ca. 8 m depth and amphiboles and micas appear ca. 14 m below the paleoweathered surface. In the Nudi (F266) profile feldspars, amphiboles and micas that are characteristic of the parent rock become dominant at a depth at about 14–15 m below the paleoweathered surface.

The kaolinite content in the uppermost ca. 1 m thick saprolite horizon reaches >55 wt% in the Varbla (502) profile, which is also developed in gneissic parent rocks. It is rapidly replaced by mixed-layer minerals and Fe-oxide phases downward in the saprock zone. K-feldspar is absent in the uppermost horizon of the saprolite section but its content increases up to 40 wt% ca. 0.6 m below the paleoweathered surface. Plagioclase is for the first time detected 4.5 m and traces of amphibole are found 6.8 m below the paleoweathered surface. The Varbla (502) profile differs from other weathering profiles by relatively high abundance of secondary carbonate minerals (calcite, dolomite and siderite) throughout the profile, which comprise up to 15 wt% (exceptionally 35 wt%) of the crystalline phases. Minor (1–2 wt%) to moderate (5–6 wt%) carbonate mineralization is also present in other weathering profiles, typically at depths >5 m (occasionally >10 m) from the paleoweathered surface (Liivamägi et al., 2015 – PAPER II).

### 4.2.2. Clay mineralogy

Clay mineralogy of the Baltic paleosol has been addressed earlier in detail in Kuuspalu et al. (1971) and Vanamb and Kirs (1990). In this thesis the composition of the clay fraction ( $<2 \mu\text{m}$ ) was analyzed in the Sigula (F124) profile to study the nature of mixed-layer clay mineral phases. In general the composition of the clay fraction agrees with the whole-rock XRD interpretation. Kaolinite (ca. 85 wt%) is a dominant clay mineral in the uppermost saprolitic zone, accompanied by mixed-layer illite–smectite (ca. 10 wt%) and by poorly crystallized illite (ca. 5 wt%). In the upper part of the saprock section the kaolinite content decreases to 10–50 wt%, whereas illite and mixed-layer illite–smectite contents increase to 10–20 wt% and 30–50 wt%, respectively. Chlorite first appears in the upper saprock section in a relatively low content between 6 and 9 wt%, and then increases up to ca. 30 wt% deeper in the saprock. Kaolinite is absent in the lower saprock section, while illite and mixed-layer illite–smectite together compose up to 10–20 wt% and chlorite (ca. 50 wt%) and mixed-layer chlorite–smectite (ca. 40 wt%) become the dominant clay phases. Previous clay mineral studies of the Baltic paleosol (Kuuspalu et al., 1971; Vanamb and Kirs, 1990) suggested the presence of smectite (montmorillonite) as the common expandable clay mineral in Baltic paleosol. However, our results suggest that expandable clay minerals are represented by different mixed-layer mineral phases – R3-ordered illite–smectite mixed-layer minerals with an expandable layer content of 15–25% in a mixed-layer structure and R1-ordered chlorite–smectite mixed-layer minerals, represented by two chlorite–smectite mixed-layer phases, with chlorite and expandable layer ratios of 49:51 or 3:97, respectively (Liivamägi et al., 2015 – PAPER II).

### 4.2.3. Scanning electron microscopy

The SEM backscattering images indicate that biotite leaching is the first sign of weathering in all the studied profiles (Pada-Aru, Sigula, Lohu and Varja). Alteration in biotite proceeds intergranularly along cleavage planes by expansion of mica flakes and subsequent replacement by Fe-oxyhydrates and chlorite–smectite-type clay phases (Figure 4a). In the weathering profiles that formed in gneissic parent rocks (e.g. Varja), plagioclase also shows the first signs of weathering already in the lower saprock section, whereas in the other profiles (Pada-Aru, Sigula and Lohu) plagioclase is preserved relatively fresh in the lower beds of the saprock. Muscovite, however, is resistant to alteration (Figure 4b) in the lower portion of all the studied weathering profiles that developed in different parent rocks (Liivamägi et al., 2015 – PAPER II).

The outlines of the original crystals are often still visible in the upper saprock section, however, when compared to the lower saprock section, the intensity of mineral dissolution has increased in the upper section and the weathering

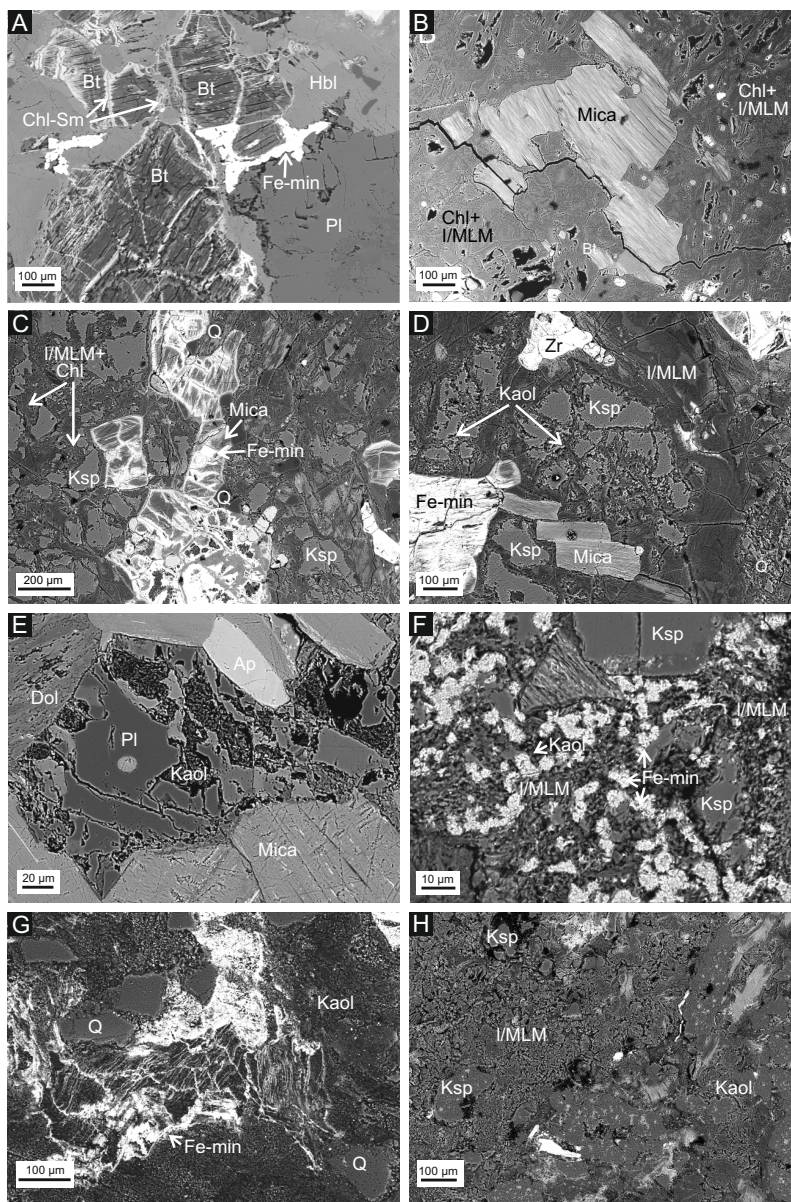


**Figure 4.** Backscattered SEM images of the Baltic paleosol profiles, developed in amphibolites–metagabbros (drillcores F185 and F280) and on gneissic basement rocks (drillcore F195). A–B: samples from lower saprock section; C–F: samples from the middle saprock section; G–H: samples from the uppermost saprolitic section. Pl – plagioclase; Bt – biotite; Hbl – hornblende; Ksp – K-feldspar; Q – quartz; Kaol – kaolinite; I/MLM – mixed layer illite–smectite; Chl – chlorite; Sm – smectite; Fe-min – hematite and/or goethite; Dol – dolomite, Ap – apatite; Zr – zircon (after Paper II – Liivamägi et al., 2015).

profile is composed of partially weathered K-feldspar, plagioclase and matrix of secondary (clay) mineral phases including kaolinite, illite, mixed-layer illite–smectite and in places chlorite and chlorite–smectite (Figure 4c–e). With increasing dissolution intensity, the K-feldspar crystals are first replaced by illite and illite–smectite in the lower saprock section (Figure 4c) and by kaolinite in the upper saprock–saprolic zone (Figure 4d). In profiles that developed in alumina-gneisses, plagioclase also shows signs of significant dissolution and is rapidly replaced by kaolinite (Figure 4e). Micas are often coated with Fe-hydroxides (hematite and goethite), while quartz and occasional zircon crystals show no signs of alteration (Figure 4c–d). Fe-minerals are not only coating partially/strongly weathered micas but are also present as larger crystalline aggregates (Figure 4d). In the weathering profiles that developed in alumina-gneisses the flake-like crystals of secondary Fe-minerals form typically radially oriented aggregates surrounded by kaolinite and illite, and mixed-layer illite–smectite phases (Figure 4f) whereas the aggregates of Fe-rich dolomite appear in the upper parts of saprock sections (Liivamägi et al., 2015 – PAPER II).

The uppermost saprolite section of the weathering profiles is characterized by fine-grained kaolinite–hematite masses embedding weathering-resistant quartz (Figure 4g) or larger kaolinite (and/or illite/mixed-layer minerals) pseudomorphs along with K-feldspar relicts (Figure 4h; Liivamägi et al., 2015 – PAPER II). The saprolite section of the Sigula (F124) profile differs from other profiles by the presence of APS minerals (Figure 5a–c). Commonly APS minerals occur as disseminated small (typically  $<2\ \mu\text{m}$ , occasionally  $5\text{--}6\ \mu\text{m}$  in size) elongated rhombohedral crystallites (Figure 5b) that are tightly inter-grown with kaolinite vermiform/booklet-like aggregates with occasional hematite flakes enclosed in APS crystals (Figure 5c). In most cases closely-packed masses of tiny APS crystallites are found in  $100\text{--}300\ \mu\text{m}$  wide patches or zones (Figure 5a), usually in the clay matrix but sometimes along edges of weathered biotite pseudomorphs and/or corroded K-feldspar remains. The crystal size of APS minerals increases and the amount of crystallites decreases downward the weathering profile where the crystallites are of pseudo-cubic form and occasionally occur as aggregates/concretions of irregular shape. Secondary apatite also occurs along with APS in deeper portions of saprolite as rims overgrowing partly dissolved/rounded apatite cores (Figure 5d) and/or as bladed-tabular euhedral to subhedral crystallites ( $10\text{--}25\ \mu\text{m}$  size) with dissolution pits often filled with kaolinite crystals (Figure 5e). Magmatic apatite cores, overgrown by secondary apatite, are typically rimmed by a thin ( $<0.2\ \mu\text{m}$  thick), most probably apatitic sheath(s) between the corroded apatite core and secondary apatite (Figure 5d). Secondary apatite and APS minerals are spatially separated in the strongly weathered clay matrix of the weathering profile and rarely occur in contact, however, in some cases secondary apatite is found embedding APS crystallites (Figure 5f), suggesting its paragenetically later formation (Virčava et al., 2015 – PAPER III).

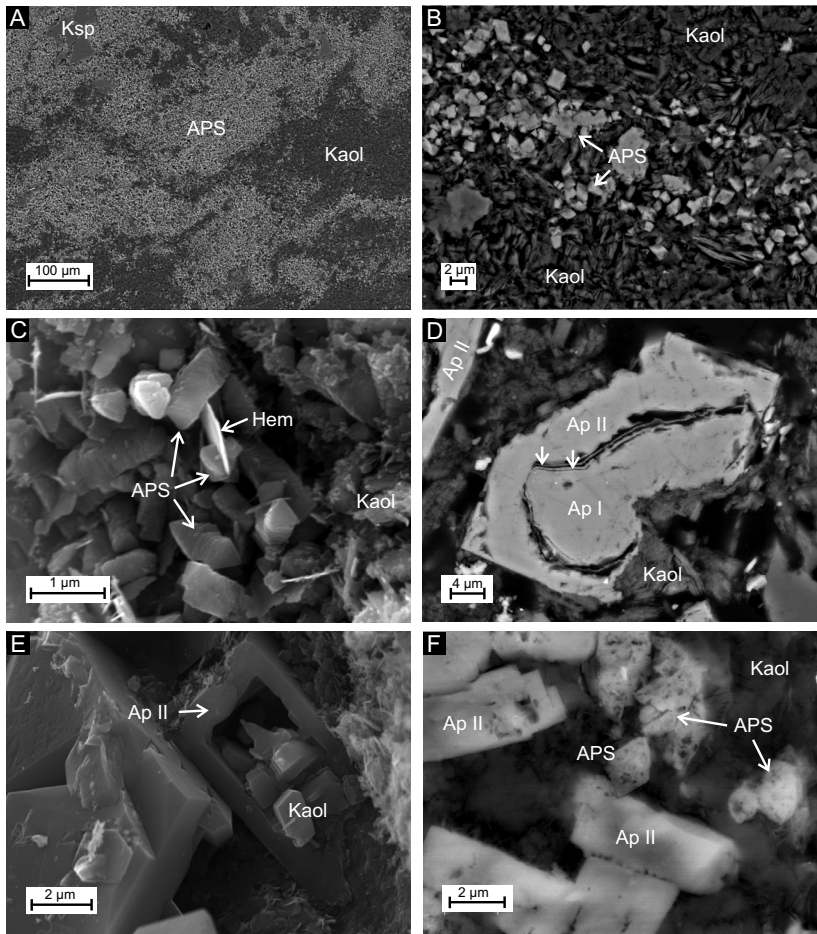


**Figure 5.** SEM images of APS mineralization and different apatite types in the Sigula (F124) weathering profile. A, C and E are from sample F124-02 and B, D and F are from sample F124-06. Images A, B, D and F were taken with backscattered electron detector, C and E with secondary electron detector. APS – aluminum phosphate–sulfate mineral, Kaol – kaolinite, Hem – hematite, Ksp – K-feldspar, Ap I – primary apatite and Ap II – secondary apatite (after Paper III – Vircava et al., 2015).

### 4.3. Geochemical characterization of the weathering profiles

Mass-balance analysis of major element enrichment-depletion (Figure 6) indicates relatively similar weathering trends in all the studied weathering profiles. Na is the most depleted element in the saprolite sections and up to 90–99% of it is lost. Mg is almost completely depleted (98–99%) in the whole 7 m thick saprolite section of the Pada-Aru (F185) profile and in the uppermost saprolite horizons (up to 98%) in other weathering profiles, except for Varja

(F195) profile where its loss is only up to 73%. Ca is also strongly depleted with volume losses up to 98% in the saprolite sections, however, it can occasionally be elevated due to the presence of secondary carbonate and/or phosphate phases. The increase in Ca, Mg and Na corresponds to the transition between saprolite and saprock zones where Ca, Mg and Na minerals such as plagioclase and amphibole appear in the mineral composition. K is strongly depleted in the uppermost saprolite sections of the Pada-Aru (F185) and Lohu (F280) profiles where volume loss is between 95 and 98% and moderately depleted in other profiles where volume loss varies greatly between 30 and 80%. K can show substantial volume gain (ca. 50–250%) in the saprock section, just below the kaolinite and Fe-rich horizons that correspond to the changes in K-feldspar, illite and illite–smectite content in the weathering profile. Al shows strong volume loss (up to 98%) in the saprolite section of Lohu (F280) profile, moderate volume loss (ca. 30%) in the Pada-Aru (F185) profile and moderate volume gain (10–40%) in the saprolite sections of other profiles. Similarly, Si shows strong volume loss (98–99%) in the saprolite section of the Lohu (F280) profile, moderate volume loss (40–70%) in the Pada-Aru (F185), Sigula (F124), Varja (F195) and Varbla (502) profiles and small volume gain (ca. 10%) in the Nudi (F266) profile. Fe is in general strongly (up to 90%) to moderately (ca. 30%) depleted in the saprolite sections of the weathering profiles. Several spikes indicating strong volume gain which do not agree with general gradually changing weathering patterns correspond to remains of coarse-grained, quartz–K-feldspar migmatite veins (Liivamägi et al., 2014, 2015 – PAPERS I, II).

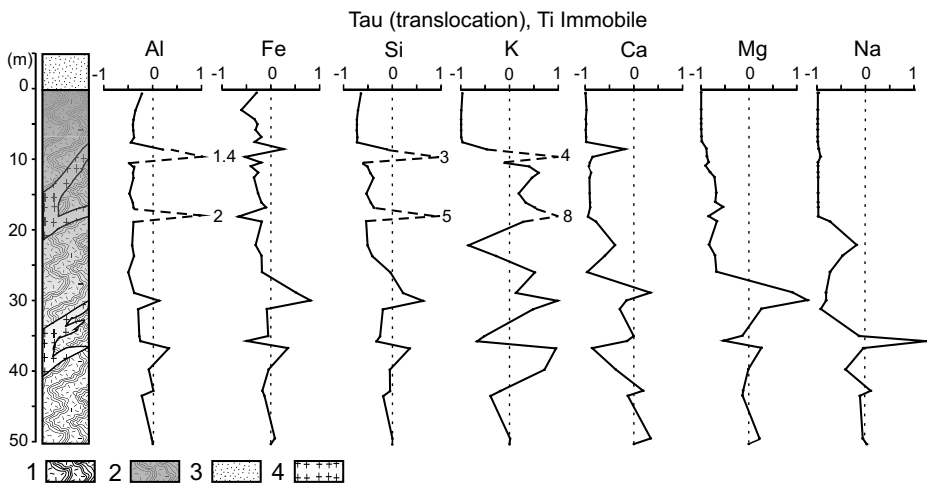


**Figure 6.** Mass-balance graph with strain (tau; translocation) of Al, Fe, Si, K, Ca, Mg, and Na versus depth of the Pada-Aru (F185) profile assuming immobile Ti. Depth is given below the paleoweathered surface. Legend: 1 – migmatized metagabbro, 2 – weathered saprock-saprolite, gray shading shows weathering intensity, 3 – Ediacaran–Cambrian sediments, 4 – coarse-grained migmatite veins (after Paper I – Liivamägi et al., 2014).



The CIA values increase from ca. 40–60 in the saprock sections up to at least 90(98) in the uppermost saprolite sections. Removing K from the index calculation causes somewhat different up-profile trends, however, in the uppermost saprolite part the CIA minus potassium (CIA – K) values still reach 98–99 in most profiles (Figure 2). The PIA values also reach >95 in the upper parts of all the studied weathering profiles (Liivamägi et al., 2015 – PAPER II). The A–CN–K plot ( $\text{Al}_2\text{O}_3 - \text{CaO} + \text{Na}_2\text{O} - \text{K}_2\text{O}$ ) shows a typical weathering trend with depletion of Ca and Na, accumulation of Al and addition of K (Figure 7; Liivamägi et al., 2014, 2015 – PAPERS I, II). The Ba/Sr (leaching) molar ratios increase in most profiles abruptly from low values up to ca. 10–30 in a depth interval ca. 5(10)–15 m below the paleoweathered surface. The Al/Si (clayey-ness) molar ratios decrease quickly from values of ca. 0.3–0.4 down to ca. 0.1–0.2 in a saprolite–saprock transition zone. The Ti/Al molar ratio (indicator of possible *in situ* weathering) shows rather uniform values between 0.03 and 0.09 in most of the Baltic paleosol weathering profiles. However, when considering the samples from altered leucosome (granitized) veins, the Ti/Al ratio can be highly variable. Positive covariations on the Zr/Al versus Zr and Ti/Al versus Ti crossplots suggest a non-uniform distribution of Ti, Zr and Al indicating heterogeneous composition of the parent material and/or translocation of clay-size material during pedogenesis (Liivamägi et al., 2015 – PAPER II).

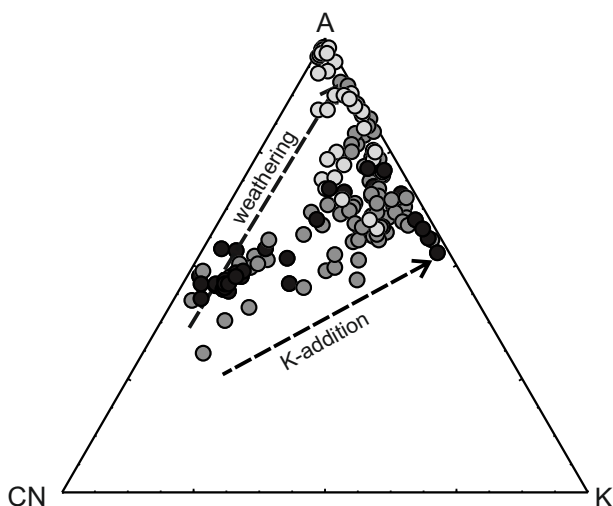


**Figure 7.** A–CN–K ( $\text{Al}_2\text{O}_3 - \text{CaO} + \text{Na}_2\text{O} - \text{K}_2\text{O}$ ) diagram with the dataset of all six weathering profiles showing an expected weathering trend and diagenetic addition of K in the Baltic paleosol. Black circles represent samples from unweathered parent rock, dark gray circles represent samples from saprock and light gray circles represent samples from saprolite (after Paper II – Liivamägi et al., 2015).

The MAT values derived from the salinization model vary between 12 and 17 °C whereas the values derived from the clayeyness model suggest higher maximum estimates ranging from 21–23 °C in the Pada-Aru (F185) profile down to 17 °C in the Nudi (F266) and Varja (F195) profiles. The MAP values obtained using the CIA – K model suggest paleoprecipitation estimates between 1300 and 1580 mm/yr and the CALMAG model suggests estimates between 1563 and 1825 mm/yr (Liivamägi et al., 2015 – PAPER II).

The chemical composition of the APS minerals in the Sigula (F124) profile shows that it is a REE- and Sr-rich and Ca-poor phase that belongs to the goyazite end-member of the APS mineral solid solutions with the crandallite component making up ca. 25%. However, in the woodhouseite–goyazite–florencite solid solution series diagram (Figure 8) its composition stays between florencite, goyazite, svanbergite and woodhouseite end-members with proportions of 0.31, 0.30, 0.18 and 0.15, respectively. Microprobe analysis of apatite cores suggests its fluoro-chloro-hydroxyl apatite composition, which is consistent with magmatic apatite in the parent rock, whereas secondary apatite has fluor- (possibly carbonate) apatite composition, characterized by a lower chlorine (<0.03 wt%) content and higher sulfur and sodium contents (Virčava et al., 2015 – PAPER III).

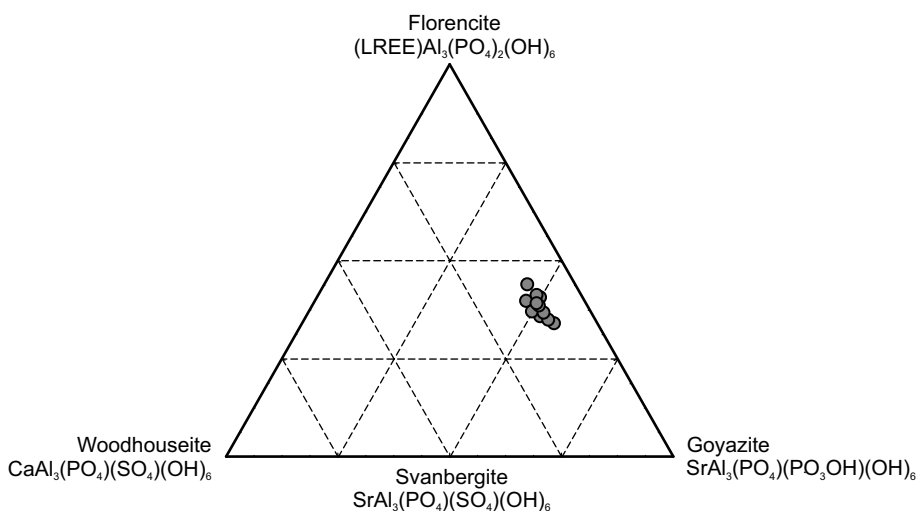


**Figure 8.** Composition of APS minerals from the Baltic paleosol in the Sigula (F124) drillcore. Ternary diagram of the florencite–woodhouseite–goyazite solid solution system. Individual circles represent the composition of single crystals or aggregates (Paper III – Virčava et al., 2015).

## 5. DISCUSSION

### 5.1. Preservation, weathering maturity and influence of diagenetic overprint

Although parent rock is heterogeneous and migmatized, the weathering profiles of Baltic paleosol are characterized by well-defined mineral alteration sequences, starting with fresh parent rock, followed by saprock and ending with clay- or sand-rich saprolite with lateritic residuum (paleosol). Whole-rock XRD and SEM analyses show that the lower saprock section is only slightly altered and the weathering of primary minerals begins with biotite replacement by chlorite and chlorite–smectite mixed-layer minerals and Fe-oxides and proceeds through the moderately weathered upper saprock section, reaching end-point in the uppermost saprolite section, which consists mainly of clays (kaolinite, illite and illite–smectite mixed-layer minerals), Fe-oxyhydroxides and residual quartz. The saprolite sections in the Varja (F195), Nudi (F266) and Varbla (502) profiles, developed in gneissic rocks, can be more accurately described as granitic saprolite because quartz grains are very abundant in the uppermost clay- (and sand-)rich zone.

These mostly reddish-colored kaolinite-dominated paleosol horizons have completely lost their original texture/structure and are abundant in Fe-oxyhydroxides. The Fe-mineral-rich zone was probably formed as a result of oxidative weathering of ore minerals and/or biotite (Sandler et al., 2012). In tropical climate the kaolinite-dominated soil profiles are frequently associated with Al-oxyhydroxide phases like gibbsite (e.g. Tardy, 1997), but neither gibbsite nor other Al-oxide-oxyhydrate phases were detected in any of the six studied weathering profiles. The absence of gibbsite may suggest poor drainage conditions for percolating meteoric water, a lowered removal rate of dissolved silica and therefore dominant precipitation of kaolinite and Fe-oxyhydrates rather than Al-oxyhydrates (Macías Vazques, 1981; Mahaney, 1990). However, gibbsite is not a common mineral in other Precambrian paleosols either (e.g. Beukes et al., 2002; Mitchell and Sheldon, 2009, 2010) and its absence more likely results from post-burial diagenetic alteration. The activity of dissolved silica ( $\text{H}_4\text{SiO}_4$ ) controls the relative stability of major weathering products such as gibbsite, kaolinite and smectite. Gibbsite is the most stable mineral under strong and aggressive leaching conditions with low silica activity, whereas kaolinite forms in soils with moderate silica activity and very low base cation activity in the soil solutions. In closed pore space during diagenesis, the activity of dissolved silica most likely rises above  $10^{-4.5}$  (Curtis and Spears, 1971) and gibbsite becomes unstable, allowing reaction with soluble silica to form stable kaolinite. As an example, Watanabe et al. (2006) showed that during a long tropical weathering in moderately drained soils, gibbsite is consumed by the formation of more stable kaolinite.

Mineral maturity indicated by MIA shows intense weathering. In four profiles out of six MIA values rise up to 100 showing nearly complete destruction of feldspars and their replacement by kaolinite and Fe-oxyhydroxides along with residual quartz. These deeply weathered sections (MIA values >85) are on average 3–6 m thick, varying from ca. 10 m in the Pada-Aru (F185) profile down to ca. 1 m in the Varbla (502) profile. High CIA (>90) and PIA (>95) values in the uppermost saprolite sections also confirm the above average maturity of the Baltic paleosol along with complete weathering of feldspar minerals (plagioclase and K-feldspar), and the formation of clay minerals. Weathering indices, and data from XRD analyses, indicate that the uppermost parts of most weathering profiles are at least partially eroded, while variable thickness of the saprolite–saprock successions can result from different depths of erosion levels or from different paleo-topographic positions of the weathering profiles. The Pada-Aru (F185) profile, located in the eastern part of the study area and developed in metagabbros, is the best-preserved and the most complete weathering profile (with the up to 10 m thick saprolite section) studied here.

Paleoweathering profiles are commonly diagenetically or hydrothermally overprinted (Maynard, 1992). Though the Baltic paleosol is macroscopically remarkably well preserved, its mineralogical composition shows that it has been affected by K-diagenetic–metasomatic overprint (Liivamägi et al., 2014, 2015 – PAPERS I, II). There is no recognizable evidence for large-scale plagioclase–K-feldspar replacement but the diagenetic influence is evident from occasional authigenic K-feldspar overgrowths on remnants of K-feldspar detrital grains within the weathered zones and from the advanced/ordered illitization of smectitic phases as indicated by the illite/smectite ratio of 76:24 in the mixed-layer mineral in the uppermost saprolite horizon. Addition of K is also well illustrated by mass-balance changes, indicating a positive volume change in the middle (upper saprock) sections of the weathering profiles, which were originally rich in smectitic clays. This is also supported by a weak correlation between CIA and CIA – K suggesting that K has not been added to the paleosol profiles as a whole, but rather into particular horizons (Liivamägi et al., 2014 – PAPER I). Smectite and disordered mixed-layer illite–smectite minerals are typical products of surficial weathering of primary silicate materials and are thermodynamically unstable, eventually recrystallizing into illite(mica) under diagenetic and/or metamorphic–metasomatic conditions (Meunier and Velde, 2004). Illitization is commonly controlled by temperature (Środoń, 1999), but also by chemical parameters such as the availability of potassium (e.g. Bauer and Velde, 1999), fluid/rock ratio (Altaner and Ylagan, 1997), composition of precursor phases (Drits et al., 2002) and the time factor (Velde and Vasseur, 1992). The Baltic Basin, hosting the Baltic paleosol, lies within an old cratonic area and has existed under an exceptionally stable tectonic regime for the last 800 Ma (Hendriks et al., 2007). The thermal alteration indices (e.g. CAI – conodont alteration index and TAI – acritarch alteration index) values  $\leq 1$  of sedimentary organic material (Nehring-Lefeld et al., 1997; Talyzina, 1998) of

Ediacaran and Paleozoic sediments overlying the Baltic paleosol suggest that the sedimentary sequence is thermally immature and has not experienced (burial) temperatures exceeding 50–70 °C. This, however, disagrees with the illite-rich composition of mixed-layer illite–smectite phases (>65% of illite layers) in these overlying sediments (including altered volcanic ash layers – bentonites), suggesting a much more advanced diagenetic grade. This advanced illitization has been explained firstly by time-dependent recrystallization at low temperatures (Kirsimäe et al., 1999; Kirsimäe and Jørgensen, 2000) and secondly as a result of combined burial and K-rich fluid-driven processes in relation to the latest phase of development of the Scandinavian Caledonides ca. 420–400 Ma (Somelar et al., 2009, 2010). Addition of K (up to 190%) compared to the original rhyolitic glass in the illitized and feldspathized Ordovician Kinnekulle bentonite bed (stratigraphically ca. 150–200 m above the weathered surface of the Baltic paleosol) is comparable to the addition of K in the Baltic paleosol (up to 250%), indicating a similar diagenetic–metasomatic overprint on the whole sedimentary sequence in the Baltic Basin. Kaolinite in the Baltic paleosol profiles and in the overlying terrigenous Ediacaran–Cambrian sediments (Raidla et al., 2006) is well preserved and does not show any signs of diagenetic kaolinite-to-dickite transformation or illitization, therefore delimiting the maximum temperature (120–140 °C) of the diagenetic–metasomatic overprint on the Baltic paleosol.

The Neoproterozoic Baltic paleosol stands out from other Proterozoic paleosols with its tens of meters thick and mature weathering profile (Liivamägi et al., 2014 – PAPER I). The Paleoproterozoic Hekpoort paleosol (Beukes et al., 2002) is a ca. 6 m thick profile located in South Africa and similarly to the Baltic paleosol, has lateritic characteristics showing laterite grading downward through saprolite into fresh basaltic Hekpoort lavas. The Ti/Al ratios from parent rock into saprolite remain constant at ca. 0.05 indicating *in situ* formation of this lateritic profile. Upper laterite and mottled zones contain up to 18 wt% Fe<sub>2</sub>O<sub>3</sub> and up to 37.5 wt% Al<sub>2</sub>O<sub>3</sub>, whereas the CIA values are between 80 and 90. However, unlike modern laterites and the Baltic paleosol, the Hekpoort paleosol is metamorphosed and kaolinite and goethite have recrystallized into pyrophyllite and hematite, respectively. Compared to the Baltic paleosol, which is affected by low-grade diagenetic K uptake (illitization of smectite) in horizons originally rich in smectitic clays, the Mesoproterozoic paleosol profiles at Good Harbour Bay and Sturgeon Falls (USA) are better preserved without significant K-metasomatism (Mitchell and Sheldon, 2009, 2010), however, they are only moderately matured as indicated by CIA values of 50–60 and clay content of 20–30 wt%. The Neoproterozoic paleoweathered profiles, recently described from ca. 582 Ma Gaskiers Formation, Newfoundland, Canada (Retallack, 2013a), are also thin and weakly developed, with CIA values reaching ca. 60. Although there is enrichment in clays in the surficial part of the paleosol, the content of clay phases stays relatively low between 30 and 40 wt% when compared to the 70 wt% of clay phases in the Baltic paleosol. Several paleosols have been

described in the succession of the Ediacaran Member of South Australia, that was recently reinterpreted from marine to lagoonal–non-marine in origin (Retallack, 2012). The continental origin of Ediacaran Member has been heavily argued (e.g. Xiao et al., 2013) and even if they are Ediacaran paleosols, they are thin (up to 1 m) and contain only little clay up to ca. 30 wt%. The weathering profiles of the Sub-Torrison Group in north-western Scotland (ca. 900 Ma) are ca. 4 and 6 m thick, and show substantial oxidation and clay formation, including chlorite, illite, illite–smectite and pedogenic smectite that is not present in the Baltic paleosol. Similarly to the Baltic paleosol, there has been significant illitization of the surface clayey horizons but the preservation of pedogenic smectite and poorly crystallized illite suggests limited burial alteration less than 120 °C (Retallack and Mindszenty, 1994).

The comparison of Precambrian paleosols such as the Baltic paleosol with modern weathering profiles is somewhat arbitrary because of different atmospheric CO<sub>2</sub> levels and the absence of land vegetation during their formation that would have promoted chemical weathering. However mass-balance changes in the Baltic paleosol are similar to modern deeply weathered tropical soil profiles that developed on plutonic–metamorphic parent rocks (e.g. Driese et al., 2007). Although modern soil taxonomy cannot be reliably used for describing the Baltic paleosol, its uppermost 1–7 m thick kaolinitic horizons are similar to the Oxisol order (Soil Survey Staff, 2010) and could be interpreted as a (paleo)Oxisol.

## **5.2. Age, paleoclimatological–paleogeographical interpretation and implications of the Baltic paleosol**

The major denudation of the Paleoproterozoic–Mesoproterozoic Svecofennian juvenile crust and formation of the sub-Cambrian peneplain in Fennoscandia took place between 1.3 and 0.8 Ga with little or no sedimentary cover development (Kohonen and Rämö, 2005). The youngest crystalline rocks affected by formation of the Baltic paleosol are ca. 600 Ma old foidic basalt flows at the top of the peneplained rapakivi granites in Latvia (Bogatikov and Birkis, 1973; Brangulis, 1985) which mark the older limit of weathering. The minimum age of weathering is defined by the age of the transgressive series of Neoproterozoic Ediacaran siliciclastic sediments that lie directly atop the weathered crystalline basement and are correlated to the Ediacaran Redkino Regional Stage in NW Russia and Kotlin Regional Stage in Estonia (Mens and Pirrus, 1997). Zircons in volcanic rocks within the Redkino succession in NW Russia have U–Pb ages of  $555.3 \pm 0.3$  Ma close to the top (Martin et al., 2000) and  $558 \pm 1$  Ma at the base (Grazhdankin, 2003) of the section. Therefore the minimum age of weathering is ca. 560–550 Ma. For those reasons, the age of the Baltic paleosol can be tentatively constrained between 600 and 560 Ma (Liivamägi et al., 2015 – PAPER II).

The petrographic and mineralogical characteristics and molecular indices of weathering of the Baltic paleosol suggest its formation in a warm and humid climate with mean annual temperatures above 17 °C and with mean annual precipitations ca. 1500 mm/year (Liivamägi et al., 2015 – PAPER II). This is consistent with warm and humid climatic conditions typically required for the development of kaolinite–Fe-oxyhydroxide-rich soil (paleosol) profiles. Gilg et al. (2013) noted that the stable isotope composition of kaolinite in large kaolin deposits in Europe, USA and elsewhere is in equilibrium with the isotope composition of weighted annual mean precipitation recorded at low-latitude (<40°) and low-altitude (<500 m) International Atomic Energy Agency stations where average MAT is 23±5 °C and MAP is 1328±844 mm/yr. This agrees well with MAT and MAP estimates for the Baltic paleosol obtained using soil climofunction models.

It is important to point out, however, that climofunctions studied here are derived from North American soil bulk-geochemistry (Sheldon et al., 2002). They are defined with certain soil types and are therefore not directly applicable to other soils or paleosols. Also, a variety of different processes, not related to MAT and MAP, may alter the geochemical composition of paleosols. For example, salinization model (Sheldon et al., 2002) was developed for arid–semiarid lowland settings and moderate formation times and therefore its suitability to the Baltic paleosol is questionable. Another problem with the salinization model is related to K-metasomatism because the model uses K in the salinization index. If we assume that all K in the uppermost kaolinitic part of the studied weathering profiles was diagenetically added, the paleotemperatures derived from the salinization model reach a theoretical useful maximum (17.3 °C). The salinization model is most likely underestimated and could be interpreted as being higher than 17 °C, at the best. The clayeyness model (Sheldon, 2006b), on the other hand, is successfully used for Quaternary (Sheldon, 2006b), Miocene (Hamer et al., 2007) and Eocene–Oligocene (Sheldon, 2009) paleo-Inceptisols. However, no real proof of its suitability for Precambrian paleosols has yet been implied.

Problems with precipitation estimates are similar, as the relationship between MAP and the CIA – K index (Sheldon et al., 2002) gives values that are close to the maximum useful upper limit and the relationship between MAP and the CALMAG model (Nordt and Driese, 2010) was developed specifically for smectite-rich Vertisols, not for kaolinite-rich Oxisols. Therefore MAT and MAP results derived from soil climofunction models should be used with caution. It is important not to overinterpret the results and one must use multiple proxies, if possible (Sheldon and Tabor, 2009). Nevertheless, high rainfall estimates indicated here with CIA – K and CALMAG models are supported by trends in the Ba to Sr molar ratio that have been used as another indicator for leaching (Sheldon, 2006a). Strong acidic/leached conditions during the formation of the Baltic paleosol are indicated by low Ba/Sr ratios at the top of the profiles with

increased ratios lower in the saprolite–saprock horizons (Liivamägi et al., 2015 – PAPER II).

The formation of the Baltic paleosol in warm and humid climate is also indicated by APS mineralization in the Sigula (F124) weathering profile. Such mineralization is a common phenomenon in weathering environments, especially in saprolitic profiles formed in tropical climate where APS minerals co-occur with kaolinite and hematite. Although their concentration is commonly low, it can reach in rare cases 60 wt% of the crystalline phases (Dill, 2001). The APS mineral composition is a sensitive environmental indicator of the pH, temperature and chemical composition of weathering, diagenetic or hydrothermal geofluids (e.g. Dill, 2001, 2003; Gall and Donaldson, 2006). The formation of APS minerals in the Baltic paleosol was most likely controlled by the dissolution of primary phosphate minerals (magmatic apatite) providing Ca and P, leaching of plagioclase providing Al, Ca and Sr and oxidation of minor sulfate phases providing S. The Sr-rich composition of APS minerals can be explained by a high content of plagioclase (50–60 vol%) in the parent rock, which is completely lost in the uppermost 5 m thick paleosol and saprolite sections (Virčava et al., 2015 – PAPER III).

The composition of APS minerals could be used as a marker for pH during the time of its precipitation (Gaboreau et al., 2005). The APS minerals in the Baltic paleosol are represented by an intermediate of florencite–goyazite–svanbergite–woodhouseite solid-solution end-members. This suggests precipitation in acidic environment (pH 5.5), which in general agrees with the acidity of modern precipitation, though the CO<sub>2</sub> levels were probably much higher at the time of Baltic paleosol formation (Virčava et al., 2015 – PAPER III). Nevertheless, the calculated equilibrium pH of rainwater in a CO<sub>2</sub>–H<sub>2</sub>O system suggests rainwater pH 5.1 at CO<sub>2</sub> concentration of 10 PAL and pH 4.6 at the concentration of 100 PAL. It is also important that in modern soils meteoric water percolating through a layer of humus-rich topsoil could become even more acidic and corrosive. However, in the absence of extensive land vegetation in the Neoproterozoic, rainwater remains the most likely and only important source of acidity (Virčava et al., 2015 – PAPER III).

At sufficiently high phosphate concentrations apatite is stable down to pH 6 (Dill, 2001). When pH of the meteoritic fluid drops below pH 6, the dissolution of apatite starts and the precipitation of APS minerals can be initiated. In the Baltic paleosol the primary magmatic apatite is totally dissolved in the uppermost 1 m thick horizon of the weathering profile. Primary apatite cores overgrown by secondary apatite appear at 1.5 m depth and then become abundant in the lower parts of the weathering profile at 4–5 m depth. The distribution of the APS minerals and secondary apatite shows a pH gradient passing from acidic (pH 5.5) in the uppermost few meters to neutral or near neutral (pH ~7) conditions at 4–5 m depth. The oxidation of sulfides and sulfur depletion down to depths of 20–30 m below the weathered surface, show on the other hand, considerable thickness of the oxidative zone. However, since the



uppermost part of the Baltic paleosol is most likely eroded, the exact position of the transition between acidic–neutral/alkaline and oxidizing–reducing zones is somewhat arbitrary (Virčava et al., 2015 – PAPER III).

The paleogeographic position of Baltica and its relation to other continents in the Precambrian is poorly understood, except for times when Baltica is considered to have been part of the Rodinia supercontinent – at low to subtropical latitudes at 1100–970 Ma, very high latitudes at 870–850 Ma, equatorial latitudes at 800–700 Ma and intermediate-to-high latitudes by 616 Ma (Walderhaug et al., 2007). Ediacaran paleomagnetic-determined locations of Baltica between 610 and 550 Ma are chaotic showing large oscillations ( $\sim 90^\circ$ ) “over the pole”, though the most likely scenario suggests that Baltica was located at high latitudes, stretching from about  $50^\circ\text{S}$  to  $75^\circ\text{S}$  at 610 Ma down to  $\sim 30^\circ\text{S}$  by 550 Ma (Meert, 2014). By the onset of the Paleozoic, 542 Ma, Baltica was positioned at  $40\text{--}50^\circ$  southerly latitudes and it did not reach tropical–equatorial latitudes until the end of the Ordovician and beginning of the Silurian (Torsvik et al., 2012). The age of the thick kaolinitic–lateritic Baltic paleosol can be constrained between 600 and 560 Ma. This, however, would suggest that the Baltic paleosol was developed in sub-humid, temperate and probably seasonal climate, though deeply weathered lateritic paleosols are typically interpreted to represent intense weathering in warm and humid, tropical climates (e.g. Retallack and Germán-Heins, 1994; Tardy, 1997; Tabor and Montañez, 2004; Meunier, 2005). Therefore, Ediacaran paleomagnetic-determined locations of the Baltica paleocontinent in the higher latitudes are in conflict with the tropical nature of the Baltic paleosol.

However, it has been discussed that the development of thick kaolinite deposits does not depend only on temperature, but also on rainfall, permeability of the parent rock and time factor (Taylor et al., 1992; Sequeira Braga et al., 2002). As an example, Gilg et al. (2013) show that Paleogene–Miocene “cool” kaolin deposits in Finland were formed at MAT’s ca.  $13\text{--}15^\circ\text{C}$  at paleolatitudes  $>50^\circ\text{N}$ . Retallack (2008, 2009, 2010), however, argues that the formation of thick bauxitic–lateritic paleosols beyond paleotropical latitudes is tied to global transient ( $<100$  kyr duration)  $\text{CO}_2$ -greenhouse events/spikes which expanded the tropical weathering zone into higher latitudes, to areas near the Arctic and Antarctic Circles. Increased  $\text{CO}_2$  abundance accelerates kaolinite genesis and the formation of deep weathering profiles (Bird et al., 1990), without the need for very long weathering or as hot and humid climate as in the tropics today.

When interpreting the formation of the seemingly tropical Baltic paleosol at high latitudes, it is important that Avigad et al. (2005) suggested that atmospheric  $\text{CO}_2$  rose in the Late Neoproterozoic–Cambrian–Ordovician as a consequence of widespread volcanism. In addition,  $\text{CO}_2$  levels reached a concentration of 0.2 bar ( $>600$  PAL) at the terminus of Precambrian Cryogenian glacial periods (Pierrehumbert, 2004; Pierrehumbert et al., 2011). The formation of the Baltic paleosol could be time-correlative to the Ediacaran Gaskiers (ca. 582 Ma) and/or Fauquier (ca. 572 Ma) glaciations (Bowring et al., 2003; Hebert et al.,

2010), although the magnitude of these glaciations did not reach the Snowball Earth stage as the oceans remained partially open or the Snowball Earth conditions remained very short (Ivanov et al., 2013).

The formation of the Baltic paleosol at ca. 560 Ma also falls into the period when the most profound and enigmatic carbon isotope anomaly occurred in the Earth's geological record – the Shuram–Wonoka isotope excursion (Grotzinger et al., 2011; Macdonald et al., 2013) characterized by low  $\delta^{13}\text{C}$  values of marine carbonates below  $-10\text{‰}$  (Burns and Matter, 1993). While causes of this anomaly are still debated (Grotzinger et al., 2011; Schrag et al., 2013), the remineralization/oxidation of a large pre-existing dissolved and/or finely particulate organic carbon (DOC) reservoir (Fike et al., 2006) or methane (Bjerrum and Canfield, 2011), and the global spike in authigenic carbonate production (Schrag et al., 2013) are favored as an explanation for the sedimentary origin of the observed negative anomaly. The intensified remineralization/oxidation of DOC and/or methane would indeed lead to an increase in atmospheric  $\text{CO}_2$  levels. Nevertheless, possible cause-and-effect relationships between the formation of the Baltic paleosol and the Shuram–Wonoka isotope excursion are very complex and speculative at best.

Kennedy et al. (2006) suggested that the increase in clay-mineral deposits in the Neoproterozoic (“Inception of the Clay Mineral Factory”) was a result of an expansion of primitive land (microbial) biota and enhanced production of pedogenic clay minerals. Tosca et al. (2010) argued that physical erosion dominated in the Late Neoproterozoic with detrital illite–muscovite phases in the sedimentary basins. Sedimentary rocks in the East European (Russian) Platform, spanning from Mesoproterozoic to Quaternary in age (Ronov et al., 1990; Hazen et al., 2013), reveal a characteristic increase in kaolinite and smectite/mixed-layer minerals that are typical pedogenic clay phases in the Ediacaran deposits across the platform. This is also supported by the composition and distribution of clay mineral phases in the clay fraction of the Ediacaran claystone–siltstone–sandstone sequence above the Baltic paleosol with a kaolinite content of ca. 20(15)–60 wt% (Viiding et al., 1983; Raidla et al., 2006). It is evident, then, that the latest Neoproterozoic (Ediacaran) siliciclastic deposits in the East European Platform (including the former Baltica continent) are characterized by highly altered clay phases typically forming under strong chemical weathering conditions. The Baltica paleocontinent was born after the Rodinia supercontinent breakup ca. 750–720 Ma (Cocks and Torsvik, 2005) and gained its independence ca. 570 Ma. Since then, up to the end of the Silurian, Baltica was one of the world's most stable Precambrian continental blocks (Cocks and Torsvik, 2005; Torsvik et al., 2012). Roughly at the same time ca. 650–515 Ma, West and East Gondwana blocks collided and the build-up of the Gondwana supercontinent (Meert and Lieberman, 2008; Torsvik et al., 2012) led to the rise of large orogenic belts and inevitably to an increase in continental weathering rates, which is the most plausible explanation for the rise of the seawater Sr-isotope ratio at the end of the Neoproterozoic (Och and Shield-

Zhou, 2012). In this sense we could interpret that the Baltic paleosol formed in a tectonically stable interior of the separated Baltica continental block allowing the formation and preservation of deep paleosol profiles while continent–continent collisions and the build-up of orogenic belts during the build-up of the Gondwana supercontinent led to intensive physical erosion with very low preservation potential for weathering profiles (e.g. Precambrian Great Unconformity; Peter and Gaines, 2012). Nevertheless, the Baltic paleosol and combined evidence from Gondwana margins (Avigad et al., 2005) and Laurentia (Peters and Gaines, 2012) suggest a strong chemical weathering in warm and humid climate at the Proterozoic–Phanerozoic boundary, regardless of paleolatitudes.

## 6. CONCLUSIONS

The petrography, mineralogy and geochemistry of six weathering profiles of the Neoproterozoic Baltic paleosol in Estonia were studied to evaluate weathering and climofunctions during the final stages of the Precambrian. The most important conclusions of this thesis are as follows:

1. Weathering profiles in the Baltic paleosol are developed in migmatized granite gneisses and amphibolites–metagabbros and are characterized by a well-defined mineral alteration sequence topping with up to 7 m thick lateritic (Oxisolic) residuum/paleosol horizon. This horizon is composed of kaolinite (>60% of mineral phases), Fe-oxyhydroxides and residual quartz.
2. The mineral maturity index (MIA) and molecular weathering indices (CIA, CIA – K and PIA) show values reaching >90 in the uppermost horizons of the paleosol, indicating intense weathering along with almost complete destruction of feldspars and their replacement by clay minerals. Weathering indices and XRD data indicate that the Pada-Aru (F185) profile, located in the eastern part of the study area and developed in metagabbros, is best preserved, while the uppermost parts of other weathering profiles are at least partially eroded.
3. While the Baltic paleosol stands out from other Proterozoic paleosols with its mature and well-preserved weathering profiles, its mineralogical composition has been affected by moderate K-diagenetic/metasomatic overprint.
4. Several meters thick kaolinite-rich paleosol profiles along with hematite- and goethite-rich Fe-duricrusts are usually interpreted as representing intense weathering in warm and humid (tropical) climate. Tropical climate is also indicated by mass-balance changes in the Baltic paleosol which are similar to modern deeply weathered tropical soil profiles and by the presence of aluminum phosphate–sulfate (APS) minerals in the uppermost saprolite horizon of the Sigula (F124) weathering profile.
6. Climofunctions, though not directly applicable to an Oxisolic paleosol of Precambrian age, suggest mean annual temperature above 17 °C and paleo-precipitation between 1300 and 1800 mm/yr during the formation of the Baltic paleosol.
7. Down-profile variation in the APS minerals and an authigenic secondary apatite allowed reconstruction of pH gradients passing from acidic (pH 5.5) environment in the uppermost few meters to (near)neutral (pH ~7) conditions 4–5 m below the paleoweathered surface. However, the position of the transition between acidic–neutral/alkaline and oxidizing/reducing zones is somewhat arbitrary because the uppermost part of the Baltic paleosol is partially eroded.

8. The interpretation of paleoclimate suggesting tropical weathering conditions is in conflict with Baltica paleopositions at high latitudes in the Late Neoproterozoic. It is possible that weathering was continuous in a stable cratonic landscape over a long period of time, allowing the formation of a deeply weathered kaolinitic paleosol at temperate climates. However, a more likely genesis scenario is that the Baltic paleosol was formed at extratropical latitudes as a consequence of episodic, high-intensity greenhouse event (or events) at the termination of the Gaskiers/Fauquier glaciations, or possibly due to global warming during the Shuram–Wonoka isotope anomaly event.

## REFERENCES

- Altaner, S.P., Ylagan, R.F., 1997. Comparison of structural models of mixed-layer illite/smectite and reaction mechanisms of smectite illitization. *Clays and Clay Minerals* 45, 517–533.
- Aplin, A.C., Matenaar, I.F., McCarty, D.K., van Der Pluijm, B.A., 2006. Influence of mechanical compaction and clay mineral diagenesis on the microfabric and pore-scale properties of deep-water Gulf of Mexico Mudstones. *Clays and Clay Minerals* 54, 500–514.
- Avigad, D., Sandler, A., Kolodner, K., Stern, R.J., McWilliams, M., Miller, N., Beyth, M., 2005. Mass-production of Cambro-Ordovician quartz-rich sandstone as a consequence of chemical weathering of Pan-African terranes: Environmental implications. *Earth and Planetary Science Letters* 240, 818–826.
- Bauer, A., Velde, B., 1999. Smectite transformation in high molar KOH solutions. *Clay Minerals* 34, 259–273.
- Beukes, N.J., Dorland, H., Gutzmer, J., Nedachi, M., Ohmoto, H., 2002. Tropical laterites, life on land, and the history of atmospheric oxygen in the Paleoproterozoic. *Geology* 30, 491–494.
- Bird, M.I., Chivas, A.R., Fyfe, W.S., Longstaffe, F.J., 1990. Deep weathering at extratropical latitudes: a response to increased atmospheric CO<sub>2</sub>, in: Bouwman, A. F. (Ed.). *Soils and the greenhouse effect*. Chichester, Wiley, pp. 383–389.
- Bjerrum, C.J., Canfield, D.E., 2011. Towards a quantitative understanding of the late Neoproterozoic carbon cycle. *Proceedings of the National Academy of Sciences of the United States of America* 108, 5542–5547.
- Bogatikov, O.A., Birkis, A.P., 1973. Precambrian magmatism in western Latvia. *Nauka, Moscow*, 138 pp. (in Russian)
- Bowring, S.A., Myrow, P., Landing, E., Ramenzani, J., 2003. Geochronological constraints on terminal Neoproterozoic events and the rise of metazoans. *National Astrobiology Institute General Meeting Abstracts* 13045, 113–114.
- Brangulis, A., 1985. Vendian and Cambrian of Latvia. *Zinatne, Riga*, 134 pp. (in Russian)
- Brasier, M.D., 1980. The Lower Cambrian transgression and glauconite-phosphate facies in Western-Europe. *Journal of the Geological Society* 137, 695–703.
- Brimhall, G.H., Lewis, C.J., Ague, J.J., Dietrich, W.E., Hampel, J., Teague, T., Rix, P., 1988. Metal enrichment in bauxites by deposition of chemically mature aeolian dust. *Nature* 333, 819–824.
- Burns, S.J., Matter, A., 1993. Carbon isotopic record of the Latest Proterozoic from Oman. *Eclogae Geologicae Helvetiae* 86, 595–607.
- Campbell, I.H., Squire, R.J., 2010. The mountains that triggered the Late Neoproterozoic increase in oxygen: The Second Great Oxidation Event. *Geochimica et Cosmochimica Acta* 74, 4187–4206.
- Cocks, L.R.M., Torsvik, T.H., 2005. Baltica from the late Precambrian to mid-Palaeozoic times: The gain and loss of a terrane's identity. *Earth-Science Reviews* 72, 39–66.
- Curtis, C.D., Spears, D.A., 1971. Diagenetic development of kaolinite. *Clays and Clay Minerals* 19, 219–227.
- Dill, H.G., 2001. The geology of aluminium phosphates and sulphates of the alunite group minerals: a review. *Earth-Science Reviews* 53, 35–93.

- Dill, H.G., 2003. A comparative study of APS minerals of the Pacific Rim fold belts with special reference to south American argillaceous deposits. *Journal of South American Earth Sciences* 16, 301–320.
- Driese, S.G., Medaris, L.G., Ren, M.H., Runkel, A.C., Langford, R.P., 2007. Differentiating pedogenesis from diagenesis in early terrestrial paleoweathering surfaces formed on granitic composition parent materials. *The Journal of Geology* 115, 387–406.
- Drits, V.A., Sakharov, B.A., Dainyak, L.G., Salyn, A.L., Lindgreen, H., 2002. Structural and chemical heterogeneity of illite-smectites from Upper Jurassic mudstones of East Greenland related to volcanic and weathered parent rocks. *American Mineralogist* 87, 1590–1606.
- Fedo, C.M., Nesbitt, H.W., Young, G.M., 1995. Unraveling the effects of potassium metasomatism in sedimentary-rocks and paleosols, with Implications for paleoweathering conditions and provenance. *Geology* 23, 921–924.
- Fike, D.A., Grotzinger, J.P., Pratt, L.M., Summons, R.E., 2006. Oxidation of the Ediacaran Ocean. *Nature* 444, 744–747.
- Gaboreau, S., Beaufort, D., Vieillard, P., Patrier, P., Bruneton, P., 2005. Aluminum phosphate-sulfate minerals associated with Proterozoic unconformity-type uranium deposits in the east alligator river uranium field, northern territories, Australia. *Canadian Mineralogist* 43, 813–827.
- Gall, Q., Donaldson, J.A., 2006. Diagenetic fluorapatite and aluminum phosphate sulfate in the Paleoproterozoic Thelon Formation and Hornby Bay Group, northwestern Canadian Shield. *Canadian Journal of Earth Sciences* 43, 617–629.
- Gilg, H.A., Hall, A.M., Ebert, K., Fallick, A.E., 2013. Cool kaolins in Finland. *Palaeogeography Palaeoclimatology Palaeoecology* 392, 454–462.
- Grant, J.A., 1986. The isocon diagram - a simple solution to Gresens' equation for metasomatic alteration. *Economic Geology* 81, 1976–1982.
- Grazhdankin, D.V., 2003. Structure and depositional environment of the Vendian Complex in the southeastern White Sea area. *Stratigraphy and Geological Correlation* 11, 313–331.
- Grotzinger, J.P., Fike, D.A., Fischer, W.W., 2011. Enigmatic origin of the largest-known carbon isotope excursion in Earth's history. *Nature Geoscience* 4, 285–292.
- Haapala, I., Rämö, O.T., Frindt, S., 2005. Comparison of Proterozoic and Phanerozoic rift-related basaltic-granitic magmatism. *Lithos* 80, 1–32.
- Halverson, G.P., Shields-Zhou, G., 2011. Chemostratigraphy and the Neoproterozoic glaciations. *Geological Record of Neoproterozoic Glaciations* 36, 51–66.
- Hamer, J.M.M., Sheldon, N.D., Nichols, G.J., 2007. Global aridity during the Early Miocene? A terrestrial paleoclimate record from the Ebro Basin, Spain. *Journal of Geology* 115, 601–608.
- Harland, W.B., 2007. Origins and assessment of snowball Earth hypotheses. *Geological Magazine* 144, 633–642.
- Hazen, R.M., Papineau, D., Leeker, W.B., Downs, R.T., Ferry, J.M., McCoy, T.J., Sverjensky, D.A., Yang, H.X., 2008. Mineral evolution. *American Mineralogist* 93, 1693–1720.
- Hazen, R.M., Sverjensky, D.A., Azzolini, D., Bish, D.L., Elmore, S.C., Hinnov, L., Milliken, R.E., 2013. Clay mineral evolution. *American Mineralogist* 98, 2007–2029.

- Hebert, C.L., Kaufman, A.J., Penniston-Dorland, S.C., Martin, A.J., 2010. Radiometric and stratigraphic constraints on terminal Ediacaran (post-Gaskiers) glaciation and metazoan evolution. *Precambrian Research* 182, 402–412.
- Hendriks, B.W.H., Donelick, R.A., O'Sullivan, P.B., Redfield, T.F., 2007. Evidence for natural, non-thermal annealing of fission tracks in apatite. *Geochimica et Cosmochimica Acta* 71, A395–A395.
- Ivanov, A.V., Mazukabzov, A.M., Stanevich, A.M., Palesskiy, S.V., Kozmenko, O.A., 2013. Testing the snowball Earth hypothesis for the Ediacaran. *Geology* 41, 787–790.
- Johnsson, M.J., 1993. The system controlling the composition of clastic sediments, in: Johnsson, M.J. & Basu, A. (Eds.). *Processes controlling the composition of clastic sediments*. Geological Society of America Special Paper 285, pp. 1–19.
- Kennedy, M., Droser, M., Mayer, L.M., Pevear, D., Mrofka, D., 2006. Late Precambrian oxygenation; inception of the clay mineral factory. *Science* 311, 1446–1449.
- Kirs, J., Puura, V., Soesoo, A., Klein, V., Konsa, M., Koppelmaa, H., Niin, M., Urtson, K., 2009. The crystalline basement of Estonia: rock complexes of the Palaeoproterozoic Orosirian and Statherian and Mesoproterozoic Calymmian periods, and regional correlations. *Estonian Journal of Earth Sciences* 58, 219–228.
- Kirsimäe, K., Jørgensen, P., 2000. Mineralogical and Rb-Sr isotope studies of low-temperature diagenesis of Lower Cambrian clays of the Baltic paleobasin of North Estonia. *Clays and Clay Minerals* 48, 95–105.
- Kirsimäe, K., Jørgensen, P., Kalm, V., 1999. Low-temperature diagenetic illite-smectite in Lower Cambrian clays in North Estonia. *Clay Minerals* 34, 151–163.
- Kohonen, J., Rämö, O.T., 2005. Sedimentary rocks, diabases, and late cratonic evolution, in: Lehtinen, M., Nurmi, P.A., Rämö, O.T. (Eds.). *Precambrian Geology of Finland: Key to the Evolution of the Fennoscandian Shield* 14, pp. 563–603.
- Koistinen, T., Klein, V., Koppelmaa, H., Korsman, K., Lahtinen, R., Nironen, M., Puura, V., Saltykova, T., Tikhomirov, S., Yanovskiy, A., 1996. Paleoproterozoic Svecofennian orogenic belt in the surroundings of the Gulf of Finland. *Special Paper of the Geological Survey of Finland* 21, 21–57.
- Kraus, M.J., 1999. Paleosols in clastic sedimentary rocks: their geologic applications. *Earth-Science Reviews* 47, 41–70.
- Kuuspalu, T., Vanamb, V., Utsal, K., 1971. About the mineralogy of the crust of weathering of the Estonian crystalline basement. *Acta et Commentationes Universitatis Tartuensis* 286, 51–164. (in Russian)
- Lahtinen, R., Nironen, M., 2010. Paleoproterozoic lateritic paleosol-ultra-mature/mature quartzite-meta-arkose successions in southern Fennoscandia intra-orogenic stage during the Svecofennian orogeny. *Precambrian Research* 183, 770–790.
- Liivamägi, S., Somelar, P., Mahaney, W.C., Kirs, J., Vircava, I., Kirsimäe, K., 2014. Late Neoproterozoic Baltic paleosol: Intense weathering at high latitude? *Geology* 42, 323–326.
- Liivamägi, S., Somelar, P., Vircava, I., Mahaney, W.C., Kirs, J., Kirsimäe, K., 2015. Petrology, mineralogy and geochemical climofunctions of the Neoproterozoic Baltic paleosol. *Precambrian Research* 256, 170–188.
- Macdonald, F.M., Strauss, J.V., Sperling, E., Halverson, G.P., Petasch, T., Narbonne, G., Johnston, D.T., Kunzmann, M., Schrag, D.P., Higgins, J.A., 2013. The stratigraphic relationship between the Shuram carbon isotope excursion, the oxygenation of Neoproterozoic oceans, and the first appearance of the Ediacara biota and bilaterian trace fossils in northwestern Canada. *Chemical Geology* 362, 250–272.



- Macías Vazquez, F., 1981. Formation of gibbsite in soils and saprolites of temperate-humid zones. *Clay Minerals* 16, 43–52.
- Mahaney, W.C., 1990. *Ice on the Equator*, Wm Caxton Ltd., Ellison Bay, Wi., 386 pp.
- Martin, M.W., Grazhdankin, D.V., Bowring, S.A., Evans, D.A.D., Fedonkin, M.A., Kirschvink, J.L., 2000. Age of Neoproterozoic bilaterian body and trace fossils, White Sea, Russia: implications for metazoan evolution. *Science* 288, 841–845.
- Maynard, J.B., 1992. Chemistry of modern soils as a guide to interpreting Precambrian paleosols. *Journal of Geology* 100, 279–289.
- Medaris Jr., L.G., Singer, B.S., Dott Jr., R.H., Naymark, A., Johnson, C.M., Schott, R.C., 2003. Late Paleoproterozoic climate, tectonics, and metamorphism in the southern Lake Superior region and Proto-North America: evidence from Baraboo Interval quartzites. *Journal of Geology* 111, 243–257.
- Meert, J.G., 2014. Ediacaran-Early Ordovician paleomagnetism of Baltica: A review. *Gondwana Research* 25, 159–169.
- Meert, J.G., Lieberman, B.S., 2008. The Neoproterozoic assembly of Gondwana and its relationship to the Ediacaran-Cambrian radiation. *Gondwana Research* 14, 5–21.
- Mens, K., Pirrus, E., 1997. Cambrian, in: Raukas, A., Teedumäe, A. (Eds.). *Geology and mineral resources of Estonia*, Estonian Academy Publishers, Tallinn, pp. 39–51.
- Meshcherskii, A.A., Kharin, G.S., Chegesov, V.K., 2003. Precambrian weathering crust of the crystalline basement in the Kaliningrad district. *Lithology and Mineral Resources* 38, 48–54.
- Meunier, A., 2005. Clays in Soils and Weathered Rocks, in: Meunier, A. (Ed.). *Clays*, Germany, Springer, pp. 231–293.
- Meunier, A., Velde, B., 2004. *Illite: Origins, Evolution and Metamorphism*. Springer-Verlag, Berlin, 286 pp.
- Mitchell, R.L., Sheldon, N.D., 2009. Weathering and paleosol formation in the 1.1 Ga Keweenawan Rift. *Precambrian Research* 168, 271–283.
- Mitchell, R.L., Sheldon, N.D., 2010. The ~1100 Ma Sturgeon Falls paleosol revisited: implications for Mesoproterozoic weathering environments and atmospheric CO<sub>2</sub> levels. *Precambrian Research* 183, 738–748.
- Narbonne, G.M., 2005. The Ediacara Biota: Neoproterozoic Origin of Animals and Their Ecosystems. *Annual Review of Earth and Planetary Sciences* 33, 421–442.
- Nedachi, Y., Nedachi, M., Bennett, G., Ohmoto, H., 2005. Geochemistry and mineralogy of the 2.45 Ga Pronto paleosols, Ontario, Canada. *Chemical Geology* 214, 21–44.
- Nehring-Lefeld, M., Modlinski, Z., Swadowska, E., 1997. Thermal evolution of the Ordovician in the western margin of the East-European Platform: CAI and R0 data. *Geological Quarterly* 41, 129–138.
- Nesbitt, H.W., Young, G.M., 1982. Early Proterozoic climates and plate motions inferred from major element chemistry of lutites. *Nature* 299, 715–717.
- Nesbitt, H.W., Young, G.M., McLennan, S.M., Keays, R.R., 1996. Effects of chemical weathering and sorting on the petrogenesis of siliciclastic sediments, with implications for provenance studies. *Journal of Geology* 104, 525–542.
- Nordt, L.C., Driese, S.G., 2010. New weathering index improves paleorainfall estimates from Vertisols. *Geology* 38, 407–410.
- Och, L.M., Shields-Zhou, G.A., 2012. The Neoproterozoic oxygenation event: environmental perturbations and biogeochemical cycling. *Earth-Science Reviews* 110, 26–57.

- Peters, S.E., Gaines, R.R., 2012. Formation of the 'Great Unconformity' as a trigger for the Cambrian explosion. *Nature* 484, 363–366.
- Pierrehumbert, R.T., 2004. High levels of atmospheric carbon dioxide necessary for the termination of global glaciation. *Nature* 429, 646–649.
- Pierrehumbert, R.T., Abbot, D.S., Voigt, A., Koll, D., 2011. Climate of the Neoproterozoic. *Annual Review of Earth and Planetary Sciences* 39, 417–460.
- Puura, V., Huhma, H., 1993. Palaeoproterozoic age of the East Baltic granulitic crust. *Precambrian Research* 64, 289–294.
- Puura, V., Vahter, R., Klein, V., Koppelmaa, H., Niin, M., Vanamb, V., Kirs, J., 1983. The crystalline basement of Estonia. Moscow, Nauka, 208 pp. (in Russian)
- Raidla, V., Kirsimäe, K., Bitjukova, L., Jõelet, A., Shogenova, A., Šliaupa, S., 2006. Lithology and diagenesis of the poorly consolidated Cambrian siliciclastic sediments in the northern Baltic Sedimentary Basin. *Geological Quarterly* 50, 11–22.
- Rämö, O.T., Huhma, H., Kirs, J., 1996. Radiogenic isotopes of the Estonian and Latvian rapakivi granite suites: new data from the concealed Precambrian of the east European craton. *Precambrian Research* 79, 209–226.
- Retallack, G.J., 1992. How to find a Precambrian paleosol, in: Schidlowski, M., Golubic, S., Kimberley, M.M., McKirdy, D.M., Trudinger, P.A. (Eds.). *Early Organic Evolution and Mineral and Energy Resources*. Springer, Berlin, pp. 16–30.
- Retallack, G.J., 2008. Cool-climate or warm-spike lateritic bauxites at high latitudes? *Journal of Geology* 116, 558–570.
- Retallack, G.J., 2009. Greenhouse crises of the past 300 million years. *Geological Society of America Bulletin* 121, 1441–1455.
- Retallack, G.J., 2010. Lateritization and bauxitization events. *Economic Geology* 105, 655–667.
- Retallack, G.J., 2012. Were Ediacaran siliciclastics of South Australia coastal or deep marine? *Sedimentology* 59, 1208–1236.
- Retallack, G.J., 2013a. Ediacaran Gaskiers Glaciation of Newfoundland reconsidered. *Journal of the Geological Society* 170, 19–36.
- Retallack, G.J., 2013b. Ediacaran life on land. *Nature* 493, 89–92.
- Retallack, G.J., Germán-Heins, J., 1994. Evidence from paleosols for the geological antiquity of rain-forest. *Science* 265, 499–502.
- Retallack, G.J., Mindszenty, A., 1994. Well preserved Late Precambrian paleosols from northwest Scotland. *Journal of Sedimentary Research* A64, 264–281.
- Rieu, R., Allen, P.A., Plotze, M., Pettke, T., 2007a. Climatic cycles during a Neoproterozoic “snowball” glacial epoch. *Geology* 35, 299–302.
- Rieu, R., Allen, P.A., Plotze, M., Pettke, T., 2007b. Compositional and mineralogical variations in a Neoproterozoic glacially influenced succession, Mirbat area, south Oman: Implications for paleoweathering conditions. *Precambrian Research* 154, 248–265.
- Ronov, A.B., Migdisov, A.A., Hahne, K., 1990. On the problem of abundance and composition of clays of the sedimentary cover of the Russian platform. *Geokhimiya* 4, 467–482.
- Sandler, A., Teutsch, N., Avigad, D., 2012. Sub-Cambrian pedogenesis recorded in weathering profiles of the Arabian-Nubian Shield. *Sedimentology* 59, 1305–1320.
- Schrag, D.P., Higgins, J.A., Macdonald, F.A., Johnston, D.T., 2013. Authigenic carbonate and the history of the global carbon cycle. *Science* 339, 540–543.

- Scott, K.M., 1987. Solid-solution in, and classification of Gossan-Derived members of the alunite-jarosite family, Northwest Queensland, Australia. *American Mineralogist* 72, 178–187.
- Sequeira Braga, M.A., Paquet, H., Begonha, A., 2002. Weathering of granites in a temperate climate (NW Portugal): granitic saprolites and arenization. *Catena* 49, 41–56.
- Sheldon, N.D., 2006a. Abrupt chemical weathering increase across the Permian-Triassic boundary. *Palaeogeography Palaeoclimatology Palaeoecology* 231, 315–321.
- Sheldon, N.D., 2006b. Quaternary glacial-interglacial climate cycles in Hawaii. *Journal of Geology* 114, 367–376.
- Sheldon, N.D., 2009. Non-marine records of climatic change across the Eocene-Oligocene transition, in: Koeberl, C., Montanari, A. (Eds.). *The Late Eocene Earth – Hothouse, Icehouse, and Impacts: Geological Society of America Special Paper 452*, pp. 241–248.
- Sheldon, N.D., Retallack, G.J., Tanaka, S., 2002. Geochemical climofunctions from North American soils and application to paleosols across the Eocene-Oligocene boundary in Oregon. *Journal of Geology* 110, 687–696.
- Sheldon, N.D., Tabor, N.J., 2009. Quantitative paleoenvironmental and paleoclimatic reconstruction using paleosols. *Earth-Science Reviews* 95, 1–52.
- Soesoo, A., Puura, V., Kirs, J., Petersell, V., Niin, M., All, T., 2004. Outlines of the Precambrian basement of Estonia. *Proceedings of the Estonian Academy of Sciences: Geology* 53, 149–164.
- Soil Survey Staff, 2010. *Keys to Soil Taxonomy*, 11th ed.: Washington, D.C., U.S. Government Printing Office, pp. 241–255.
- Somelar, P., Kirsimäe, K., Hints, R., Kirs, J., 2010. Illitization of early Paleozoic K-bentonites in the Baltic Basin: Decoupling of burial- and fluid-driven processes. *Clays and Clay Minerals* 58, 388–398.
- Somelar, P., Kirsimäe, K., Šrodoň, J., 2009. Mixed-layer illite-smectite in the Kinnekulle K-bentonite, northern Baltic Basin. *Clay Minerals* 44, 455–468.
- Šrodoň, J., 1999. Use of clay minerals in reconstructing geological processes: recent advances and some perspectives. *Clay Minerals* 34, 27–37.
- Sutton, S.J., Maynard, J.B., 1996. Basement unconformity control on alteration, St. Francois Mountains, SE Missouri. *Journal of Geology* 104, 55–70.
- Tabor, N.J., Montañez, I.P., 2004. Morphology and distribution of fossil soils in the Permo-Pennsylvanian Wichita and Bowie Groups, north-central Texas, USA: implications for western equatorial Pangean palaeoclimate during icehouse-greenhouse transition. *Sedimentology* 51, 851–884.
- Talyzina, N.M., 1998. Fluorescence intensity in Early Cambrian acritarchs from Estonia. *Review of Palaeobotany and Palynology* 100, 99–108.
- Tardy, Y., 1997. *Petrology of Laterites and Tropical Soils*. Rotterdam, Balkema, 408 pp.
- Taylor, J.C., 1991. Computer programs for standardless quantitative analysis of minerals using the full powder diffraction profile. *Powder Diffraction* 6, 2–9.
- Taylor, G., Eggleton, R.A., Holzhauser, C.C., Maconachie, L.A., Gordon, M., Brown, M.C., McQueen, K.G., 1992. Cool climate lateritic and bauxitic weathering. *The Journal of Geology* 100, 669–677.
- Torsvik, T.H., Van der Voo, R., Preeden, U., Mac Niocaill, C., Steinberger, B., Doubrovine, P.V., van Hinsbergen, D.J.J., Domeier, M., Gaina, C., Tohver, E.,

- Meert, J.G., McCausland, P.J.A., Cocks, L.R.M., 2012. Phanerozoic polar wander, palaeogeography and dynamics. *Earth-Science Reviews* 114, 325–368.
- Tosca, N.J., Johnston, D.T., Mushegian, A., Rothman, D.H., Summons, R.E., Knoll, A.H., 2010. Clay mineralogy, organic carbon burial, and redox evolution in Proterozoic oceans. *Geochimica et Cosmochimica Acta* 74, 1579–1592.
- Vanamb, V., Kirs, J., 1990. Clay minerals from aluminous gneiss weathering crust of the Estonian crystalline basement. *Acta et Commentationes Universitatis Tartuensis* 885, 23–37. (in Russian)
- Velde, B., Vasseur, G., 1992. Estimation of the diagenetic smectite to illite transformation in time-temperature space. *American Mineralogist* 77, 967–976.
- Viiding, H., Konsa, M., Kleesment, A., Heinsalu, H., Jürgenson, E., 1983. Evolution of the temgenous component of sedimentary rocks of the southern slope of the Baltic Shield, in: Viiding H. (Ed.). *Terrigenous minerals of the Baltic sedimentary rocks*, pp. 7–22. (in Russian)
- Vircava, I., Somelar, P., Liivamägi, S., Kirs, J., Kirsimäe, K., 2015. Origin and paleoenvironmental interpretation of aluminum phosphate–sulfate minerals in a Neoproterozoic Baltic paleosol. *Sedimentary Geology* 319, 114–123.
- Walderhaug, H.J., Torsvik, T.H., Halvorsen, E., 2007. The Egersund dykes (SW Norway): A robust Early Ediacaran (Vendian) palaeomagnetic pole from Baltica. *Geophysical Journal International* 168, 935–948.
- Watanabe, T., Funakawa, S., Kosaki, T., 2006. Clay mineralogy and its relationship to soil solution composition in soils from different weathering environments of humid Asia: Japan, Thailand and Indonesia. *Geoderma* 136, 51–63.
- Xiao, S.H., Droser, M., Gehling, J.G., Hughes, I.V., Wan, B., Chen, Z., Yuan, X.L., 2013. Affirming life aquatic for the Ediacara biota in China and Australia. *Geology* 41, 1095–1098.

## SUMMARY IN ESTONIAN

### Neoproterosoilise Balti paleomurenemiskooriku geoloogia ja paleokeskkonna analüüs

Murenemiskoorikute mineraloogilis-geokeemiline koostis sõltub lähtekivimist ning murenemisaegsetest kliimaatilistest tingimustest. Seetõttu on nende kvalitatiivne ja kvantitatiivne analüüs leidnud laialdast kasutust paleokliima rekonstrueerimisel (Sheldon ja Tabor 2009). Eelkambriumi enam kui 550 miljoni aasta vanused murenemiskoorikud on haruldased, tüüpiliselt moondunud ja/või mõjutatud hüdrotermaalsetest protsessidest, kuid siiski pakuvad nad erilist tähelepanu varajase Maa keskkondade uurimiseks (Retallack 1992). Vahetult enne Proterosoikumi–Paleosoikumi piiri *ca.* 550 miljonit aastat tagasi toimusid lühiajalised, kuid suureamplituudilised muutused süsinikuringes, hapniku sisaldus Maa atmosfääris kasvas tänapäevasele tasemele, toimusid globaalsed jäätmised, millele järgnesid lühiajalised nn kasvuhoonekliimaga perioodid, ja ilmusid esimesed hulkraksed loomad, mis tähistas bioloogilise mitmekesisuse plahvatusliku arengu algust (Narbonne 2005, Harland 2007, Pierrehumbert jt 2011). Kuigi Eelkambriumi kontinentaalsed murenemissündmused on säilinud pigem kulutuspeelade kui terviklike murenemiskoorikutena (Peters ja Gaines 2012), siis Ida–Euroopa platvormi kristalsel aluskorral Eestis, Lätis, Leedus ja Loode-Venemaal on säilinud mitmekümne meetri paksune Neoproterosoikumiaegne murenemiskoorik. Käesoleva doktoritöö eesmärkideks oli selgitada Balti murenemiskooriku petrograafiline ning mineraloogilis-geokeemiline koostis kuues puursüdamikes avatud läbilõikes (Varja, Pada-Aru, Nudi, Sigula, Lohu ja Varbla), et hinnata murenemiskooriku säilivust, murenemisastet, võimalikke hilisdiageneetilisi ja hüdrotermaalseid mõjutusi, ning rekonstrueerida paleokliimaatilised tingimused murenemiskooriku moodustumise ajal.

Eesti kristalne aluskord on tekkinud Svekofenni orogeneesi käigus ja koosneb peamiselt 1,9–1,7 miljardi aasta vanustest keskmise ja kõrge moondeastmega meta-settekivimitest (Kirde-Eesti) ja meta-vulkaanilistest (Lääne- ja Lõuna-Eesti) kivimitest, mida läbib 1,6–1,4 miljardi aasta vanused postorogeensed (rabakivi) graniidi intrusioonid (Haapala jt 2005, Kirs jt 2009). Svekofenni mäetekkele järgnes mandriline kulutusperiood, mille tulemusena kujunes laiaulatuslik murenemiskoorik, mida katavad põikselte ligikaudu 560–550 miljoni aasta vanused Ediacara ja Kambriumi setted (Puura jt 1983, Mens ja Pirrus 1997). Noorimad murenemisest mõjutatud kristalse aluskorra kivimid on ligikaudu 600 miljoni aasta vanused aluselised ja ultraaluselised laavad Ida-Lätis (Bogatikov ja Birkis 1973, Brangulis 1985). Seega kujunes Balti murenemiskoorik hinnanguliselt 600–560 miljonit aastat tagasi.

Kuigi Balti murenemiskoorik on teiste omavanuste murenemiskoorikutega võrreldes väga hästi säilinud, viitab selle tsonaalsus murenemiskooriku kulutatusele. Sügavama erosioonilõike puhul puuduvad murenemiskooriku läbilõikes kas täielikult või osaliselt kõrgema murenemisastmega (saproliidi) tsoonid.

Uuritud profiilidest on kõige paremini säilinud Pada-Aru (F185) läbilõige, kus on esindatud ka kõige enam muutunud kaoliniitsed–hematiitsed ülemised tsoonid. Mineraloogilised analüüsid näitavad, et murenemine saab alguse juba välise ilme järgi värskes kivimis, kus vilkude/biotiidi mikrolõhedes hakkab toimuma asendumine sekundaarsete savimineraalide ja Fe-oksühüdraatsete massidega. Erinevate keemiliste ja mineraloogiliste murenemisindeksite kõrged väärtused (>90) viitavad päevakivide täielikule lahustumisele ja asendumisele erinevate savimineraalidega. Balti murenemiskooriku kõige ülemises, kõrge murenemisastmega osas on domineerivaks (savi)mineraaliks kaoliniit (>60 %) koos hematiidi/götiidi ja murenemisele vastupidava nn jääkkvartsiga. Keskmise murenemisastmega tsoonides on savimineraalide kooslus esindatud segakihiliste illiit–smektiidi ja kloriit–smektiidiga ning madalaima murenemisastmega osades kloriidi ja segakihilise kloriit–smektiidiga. Geokeemilised analüüsid ja massitasakaalu arvutused näitavad, et murenemisel vähe leostuva/liikuva Ti suhtes on murenemisprofiilide ülemised, tugevalt leostunud osad kõige enam vaesustunud Na, Mg ja Ca suhtes ning võrreldes murenemise lähtekivimiga on 90–99% nendest elementidest välja kantud. K on samuti kõrgeima murenemisastmega tsoonis peaaegu täielikult kadunud, kuid keskmise murenemisastmega tsooni iseloomustab võrreldes lähtekivimiga järsk K sisalduse kasv (50–250%), mis viitab selle, algselt smektiidirikka murenemiskooriku tsooni illitiseerumisele (Somelar 2009, 2010), kuid kuna kaoliniit ei ole illitiseerumisest mõjutatud, võib järeldada, et selle mõju Balti murenemiskoorikule on olnud vähene.

Suure, mitmekümne meetri paksusega Al (kaoliniidi) ja Fe (hematiidi/götiidi) oksiidide/oksühüdroksiidide rikast punase värvusega murenemiskoorikut seostatakse tavaliselt lateriidistumise ja kuuma/niiske troopilise kliimaga. Sellist Balti murenemiskooriku tekkekeskkonna tõlgendust toetavad ka murenemisindeksite väärtustest lähtuvad paleotemperatuuride ja -sademete hinnangud, mis viitavad aasta keskmisele temperatuurile >17 °C ja aasta keskmisele sademete hulgale 1300–1800 mm/aastas. Siinkohal on oluline arvestada, et erinevad murenemisindeksid on välja töötatud kaasaegsetes, pigem mõõduka kliimaga ja/või tugeva aastaegade (sademete) kontrastiga mullatekke keskkondades ning nende kasutamine Eelkambriumivanuste, troopilistes tingimustes moodustunud murenemiskoorikute tõlgendamiseks on tihti küsitav ja vajab võimalusel täiendavaid ning sõltumatuid argumente. Samas, Balti murenemiskooriku troopilist iseloomu toetab ka APS (alumiinium fosfaat–sulfaat) mineraalide esinemine Sigula (F124) murenemisprofiili kõige ülemises, kõrge murenemisastmega osas, kus selle uustekkelise mineraali osakaal ulatub 4%-ni. APS mineraalide esinemine koos uustekkelise apatiidiga võimaldab hinnata ka murenemiskeskonna pH-d. APS mineralisatsiooni ja uustekkelise apatiidi esinemise alusel võib oletada, et happeline (pH~5) ning tugevalt leostunud tsoon ulatus 1–2 meetri sügavusele murenemiskooriku pinnast kuni neutraalse keskkonnani (pH~7) ligikaudu 4–5 meetri sügavusel.

Nii mineraloogiliste kui geokeemiliste analüüside tulemused viitavad, et Balti (lateriitne) murenemiskoorik kujunes tugeva leostumise tagajärjel soojas ja niiskes kliimas. Selline tõlgendus on vastuolus Baltika paleokontinendi asukohaga kõrgetel laiuskraadidel (<40) ja valitsevate parasvöötme kliimatingimustega 600–560 miljonit aastat tagasi. Kuigi kaoliniitne murenemiskoorik võib kujuneda ka pika aja jooksul, keskmisest kõrgema sademetehulga ja mõõduka temperatuuriga kliimas, siis on tõenäolisem, et Balti murenemiskoorik kujunes lühiajaliselt intensiivistunud murenemise tulemusena vahetult enne Ediacara mere pealetungi *ca.* 560 miljonit aastat tagasi. Intensiivistunud murenemise võisid põhjustada (globaalsetele?) jäätumistele järgnenud nn kasvuhoooneperioodid või süsinikuringe suureskaalalise anomaalia põhjustanud Shuram-Wonoka sündmus, mille tagajärjel järsult ja geoloogilises mõttes lühiajaliselt (<10 miljoniks aastaks) tõusnud atmosfääri CO<sub>2</sub> sisaldus põhjustas sademete hapestumise ning võimaldas lateriitse murenemiskooriku kujunemist lühikese aja jooksul ka kõrgetel laiuskraadidel väljaspool troopilist kliimavöödet.

## **ACKNOWLEDGEMENTS**

Above all I am grateful to my supervisors Kalle Kirsimäe and Peeter Somelar whose help and guidance throughout my PhD studies is highly appreciated.

I would also like to thank Jaan Aruväli who helped me with XRD and XRF analyses and my co-authors Juho Kirs, Ilze Vircava and William C. Mahaney. All my other colleagues and friends from the University of Tartu, Department of Geology are thanked as well, especially everyone from the room 3005.

Anne Noor and Karin Veske are acknowledged for language correction.

Financial support from the Estonian Ministry of Education and Research (grant SF0180069s08) and Estonian Research Council (grants 8744, 9196, ERMOS100, IUT20-34 and PUT762), Doctoral School of Earth Sciences and Ecology and Archimedes Foundation (Kristjan Jaak Scholarship) are gratefully acknowledged.

Finally, my sincerest thanks go to my family and friends for their encouragement and support.



## **PUBLICATIONS**

# CURRICULUM VITAE

**Name:** Sirle Liivamägi  
**Date of birth:** 09.09.1986  
**Address:** Department of Geology, University of Tartu,  
Ravila 14a, 50411 Tartu, Estonia  
**Contact:** Phone +372 5275375  
**E-mail:** sirle.liivamagi@ut.ee

## Education

2010–... University of Tartu, Department of Geology  
PhD student in Geology  
2008–2010 University of Tartu, MSc in Geology  
2005–2008 University of Tartu, BSc in Geology  
2002–2005 Tallinn Laagna Gymnasium

## Professional employment

2012–2014 Data analysis specialist,  
University of Tartu, Department of Geology

## Research activity

Field of research:  
geochemistry, mineralogy, clay mineralogy, Precambrian, chemical weathering,  
paleosols

## Publications

- Vircava, I., Somelar, P., **Liivamägi, S.**, Kirs, J., Kirsimäe, K., 2015. Origin and paleoenvironmental interpretation of aluminum phosphate–sulfate minerals in a Neoproterozoic Baltic paleosol. *Sedimentary Geology* 319, 114–123.
- Liivamägi, S.**, Somelar, P., Vircava, I., Mahaney, W.C., Kirs, J., Kirsimäe, K., 2015. Petrology, mineralogy and geochemical climofunctions of the Neoproterozoic Baltic paleosol. *Precambrian Research* 256, 170–188.
- Liivamägi, S.**, Somelar, P., Mahaney, W.C., Kirs, J., Vircava, I., Kirsimäe, K., 2014. Late Neoproterozoic Baltic paleosol: Intense weathering at high latitude? *Geology* 42, 323–326.

## ELULOOKIRJELDUS

**Nimi:** Sirle Liivamägi  
**Sünniaeg:** 09.09.1986  
**Address:** Geoloogia osakond, Tartu Ülikool,  
Ravila 14a, 50411 Tartu, Eesti  
**Kontakt:** Tel. +372 5275375  
**E-post:** sirle.liivamagi@ut.ee

### Haridus

2010–... Tartu Ülikool, Geoloogia osakond, geoloogia doktorant  
2008–2010 Tartu Ülikool, MSc geoloogias  
2005–2008 Tartu Ülikool, BSc geoloogias  
2002–2005 Tallinna Laagna Gümnaasium

### Teenistuskäik

2012–2014 Andmetöötuse spetsialist,  
Tartu Ülikool, Geoloogia osakond

### Teadustegevus

Teadustöö põhisuunad:

geokeemia, mineraloogia, savimineraloogia, Eelkambrium, keemilised murenemisprotsessid, murenemiskoorikud

### Publikatsioonid

- Vircava, I., Somelar, P., **Liivamägi, S.**, Kirs, J., Kirsimäe, K., 2015. Origin and paleoenvironmental interpretation of aluminum phosphate–sulfate minerals in a Neoproterozoic Baltic paleosol. *Sedimentary Geology* 319, 114–123.
- Liivamägi, S.**, Somelar, P., Vircava, I., Mahaney, W.C., Kirs, J., Kirsimäe, K., 2015. Petrology, mineralogy and geochemical climofunctions of the Neoproterozoic Baltic paleosol. *Precambrian Research* 256, 170–188.
- Liivamägi, S.**, Somelar, P., Mahaney, W.C., Kirs, J., Vircava, I., Kirsimäe, K., 2014. Late Neoproterozoic Baltic paleosol: Intense weathering at high latitude? *Geology* 42, 323–326.

## DISSERTATIONES GEOLOGICAE UNIVERSITATIS TARTUENSIS

1. **Пэп Мянник.** Конодонты в верхнеордовикских и нижнесилурийских отложениях Эстонии. Тарту, 1992, 355 с.
2. **Elvi Tavast.** Fennoskandia kilbi lõunanõlva ja sellega piirnevate alade aluspõhja reljeef. Tartu, 1992, 357 lk.
3. **Kaarel Orviku.** Characterisation and evolution of Estonian seashores. Tartu, 1992, 19 p.
4. **Анатолий Молодьков.** ЭПР-анализ скелетного вещества моллюсков в хроностратиграфических исследованиях позднего кайнозоя. Тарту, 1992, 33 с.
5. **Jaan Lutt.** Late- and postglacial deposits on the Estonian shelf. Tartu, 1993, 31 p.
6. **Reet Karukäpp.** Gotiglatsiaalne morfogenees Skandinaavia mandriliustiku kagusektoris. Tartu, 1997, 181 p.
7. **Argo Jõelett.** Geothermal studies of the Precambrian basement and Phanerozoic sedimentary cover in Estonia and Finland. Tartu, 1998, 125 p.
8. **Jüri Nemliher.** Mineralogy of Phanerozoic skeletal and sedimentary apatites: an XRD study. Tartu, 1999, 134 p.
9. **Kalle Kirsimäe.** Clay mineral diagenesis on the Lower Cambrian “Blue Clay” in the northern part of the Baltic Paleobasin. Tartu, 1999, 113 p.
10. **Jüri Plado.** Gravity and magnetic signatures of meteorite impact structures. Tartu, 2000, 87 p.
11. **Olev Vinn.** Morphogenesis and phylogenetic relationships of Clitambonitidines, Ordovician Brachiopods. Tartu, 2001, 127 p.
12. **Leho Ainsaar.** The middle Caradoc facies and faunal turnover in the late Ordovician Baltoscandian palaeobasin: sedimentological and carbon isotope aspects. Tartu, 2001, 109 p.
13. **Oive Tinn.** Early Ostracode evolution and Palaeoenvironmental application in the Ordovician of Baltoscandia. Tartu, 2002, 145 p.
14. **Maris Rattas.** Subglacial environments in the formation of drumlins — The case of the Saadjärve Drumlin Field, Estonia. Tartu, 2004, 117 p.
15. **Ene Kadastik.** Upper-Pleistocene stratigraphy and deglaciation history in northwestern Estonia. Tartu, 2004, 129 p.
16. **Helje Pärnaste.** Early Ordovician trilobites of suborder Cheirurina in Estonia and NW Russia: systematics, evolution and distribution. Tartu, 2004, 138 p.
17. **Mari-Ann Mõtus.** Silurian (Llandovery-Wenlock) tabulate corals of Baltoscandia: taxonomy, palaeoecology, distribution. Tartu, 2005, 167 p.
18. **Alar Rosentau.** Development of proglacial lakes in Estonia. Tartu, 2006, 114 p.

19. **Evelin Verš.** Development of impact-induced hydrothermal system at Kärđla impact structure. Tartu, 2006, 96 p.
20. **Sigitas Radzevičius.** The genus *Pristiograptus* in Wenlock of East Baltic and the Holy Cross Mountains. Tartu, 2007, 133 p.
21. **Andres Marandi.** Natural chemical composition of groundwater as a basis for groundwater management in the Cambrian-Vendian aquifer system in Estonia. Tartu, 2007, 116 p.
22. **Eve Niinemets.** Vegetation and land-use history of the Haanja Heights (SE-Estonia) during the Holocene. Tartu, 2008, 146 p.
23. **Kalle-Mart Suuroja.** Geology and lithology of the early Palaeozoic marine impact structures Kärđla and Neugrund (Estonia). Tartu, 2008, 234 p.
24. **Rutt Hints.** Early diagenesis of Ordovician and Silurian Bentonites in the Northern Baltic Palaeobasin. Tartu, 2009, 90 p.
25. **Peeter Somelar.** Illitization of K-bentonites in the Baltic Basin. Tartu, 2009, 118 p.
26. **Ulla Preeden.** Remagnetizations in sedimentary rocks of Estonia and shear and fault zone rocks of southern Finland. Tartu, 2009, 121 p.
27. **Kati Tänavsuu-Milkeviciene.** Transgressive to regressive turnaround in the Middle Devonian Baltic Basin. Tartu, 2009, 106 p.
28. **Valle Raidla.** Chemical and isotope evolution of groundwater in the Cambrian-Vendian aquifer system in Estonia. Tartu, 2010, 134 p.
29. **Kadri Sohar.** Quaternary ostracods from Estonia and their application in palaeoenvironmental reconstruction. Tartu, 2010, 140 p.
30. **Kristjan Urtson.** Stepwise melt transport and accumulation: analogue and numerical modelling approach. Tartu, 2011, 83 p.
31. **Marko Kohv.** Landslides in clayey soils of western Estonia. Tartu, 2011, 116 p.
32. **Nele Muttik.** Post-impact alteration of impactites: Ries crater, Germany. Tartu, 2011, 78 p.
33. **Annette Sedman.** Strength and self-cementing properties of oil shale retorting wastes. Tartu, 2013, 82 p.
34. **Arkady Tsyruľnikov.** Complex seismo-acoustic and lithological study of the Lateglacial and postglacial sediments northern Gulf of Riga, eastern branch of the central Baltic Sea. Tartu, 2013, 102 p.
35. **Marge Uppin.** Geological sources and hydrochemistry of fluoride and boron in Silurian-Ordovician aquifer system. Tartu, 2013, 86 p.
36. **Peeter Talviste.** Temporal changes in weak natural and artificial soils – influence on geotechnical characteristics. Tartu, 2014, 204 p.
37. **Katrin Lasberg.** Chronology of the Weichselian Glaciation in the south-eastern sector of the Scandinavian Ice Sheet. Tartu, 2014, 100 p.